IEEE Access
Multidisciplinary | Rapid Review | Open Access Journal

Received February 20, 2020, accepted February 28, 2020, date of publication March 3, 2020, date of current version March 12, 2020.

Digital Object Identifier 10.1109/ACCESS.2020.2977986

Output Feedback Spatial Trajectory Tracking Control of Underactuated Unmanned Undersea Vehicles

HAOMIAO YU[1], CHEN GUO[1], ZHIPENG SHEN[1], AND ZHEPING YAN[2]
[1]College of Marine Electrical Engineering, Dalian Maritime University, Dalian 112016, China
[2]College of Automation, Harbin Engineering University, Harbin 150001, China

Corresponding author: Haomiao Yu (yuhaomiao1983@163.com)

This work was supported in part by the National Natural Science Foundation of China under Grant 51809028, Grant 51879027, and Grant 51579024, in part by the Doctoral Start-up Foundation of Liaoning Province under Grant 2019-BS-022, and in part by the Fundamental Research Funds for the Central Universities under Grant 3132019109 and Grant 3132019318.

ABSTRACT In this paper, suffering from both parameter perturbation and unknown ocean currents, the spatial trajectory tracking problem of an underactuated unmanned undersea vehicle (UUV) is investigated in the absence of full state information. The equivalent output injection sliding mode observer is applied to estimate the linear and angular velocities of underactuated UUVs in finite time. Meanwhile, the spatial trajectory tracking controller is developed based on the bioinspired filtering backstepping technique and integral sliding mode control principle, which guarantees to steer the underactuated UUV to track the desired trajectory and stabilizes all tracking errors to the bounded neighborhood of the origin. Numerical simulation results are presented and analyzed to demonstrate the preferably control performance of the proposed tracking control scheme.

INDEX TERMS Adaptive sliding mode observer, output feedback, parameter perturbation, spatial trajectory tracking, underactuated UUV.

I. INTRODUCTION

In recent years, the control problems of underactuated unmanned undersea vehicles (UUVs) have been the hot topic in the marine engineering [1]–[8]. These attentions originate from huge theoretical challenges arising from highly nonlinear, parameter perturbation, unmeasurable velocities and unknown environmental disturbances [2]–[4], [9], [10], and a wide range of the applications including exploration and exploitation of resources locating at deep oceanic environments, geological sampling, oceanographic observation, search and inspection of underwater structures, intelligence/surveillance/reconnaissance (ISR) and anti-submarine warfare (ASW) [1], [11], [12]. The motion control technique of underactuated UUVs is necessary and prerequisite for successfully and efficiently performing various complex missions. In practice, for decreasing the cost and weight of UUVs, they are configured to underactuated mode.

The number of motion-control actuator for underactuated UUVs is fewer than degrees-of-freedom (DOF). For the UUV type considered in this work, the one is equipped with only three independent motion-control actuators, namely a pair of the identical stern thrusters, a pair of sternplanes and a pair of rudders, which are mounted symmetrically in the aft. It is clear that the research object of this article belongs to a class of underactuated mechanical systems with second-order nonholonomic constraints and drift items [13], [14]. The underactuated UUVs are not stabilized by any smooth or continuous time-invariant feedback controllers, in the light of the famous Brockett's necessary condition [15], [16]. Therefore, the trajectory tracking control problem of underactuated UUVs is extremely challenging and great meaningful, which is a hot and active research topic [3]–[11], [17]–[30].

Generally speaking, the traditional trajectory tracking control algorithms of marine vehicles (including ship, submarine, USV, UUV, ROV and so on) are developed under the condition that all the motion states are measurable. These full state feedback tracking controllers are proposed based on numerous nonlinear control methods, such as backstepping technique [3], [8], [17], [18], [24], [25], [29], Lyapunov's direct method [3], [17], [18], sliding mode control (SMC) [4], [10], [20], [23]–[26], [31], [32], adaptive control

The associate editor coordinating the review of this manuscript and approving it for publication was Shihong Ding.

[17]–[19], [26], [27], etc. All the aforementioned control schemes require that all states of marine vehicles are measurable, including the linear and angular velocities in the body-fixed reference frame and the position and attitude in the inertial reference frame. The motion states of underwater vehicles can be measured by sensors and navigation, such as the position and attitude of undersea vehicles measured by the inertial navigation system (INS) and their linear velocities measured by the Doppler velocity log (DVL) [9], [33]. Specifically, the type localization systems of undersea vehicles typically comprise the navigation satellite system (GPS/GLONASS/BDS), acoustic positioning system (USBL/SBL/LBL/PLBL/UTP), inertial navigation system (SINS/PHINS), and geophysical navigation [2]. However, these navigation equipment can only be partially equipped with UUVs, due to total mass or cost limitations. In particular, low-cost UUVs can hardly be equipped with expensive SINS and DVL. According to the principle of DVL, its measurement may be invalid due to change in seabed topography or sea state. In addition, the angular velocities are difficult to measure accurately by existing sensors. All of these reasons will cause those full state feedback trajectory tracking control scheme to fail.

Over the last decade, many scholars have gradually begun to care about the output feedback trajectory tracking problems [34]–[38]. S. Li et al. proposed a finite-time output feedback trajectory tracking controller of full-actuated UUVs based on the fractional power integrator approach [9]. Y. Wang et al. addressed the output tracking problem of ROV in 4-DOF using nonsingular terminal sliding mode [21], [36]. Reference [39], authors addressed the output feedback trajectory tracking problem of underactuated ships based on high-gain observer, parameter compression algorithm and performance function. Among the above research results, there are not the output feedback spatial trajectory tracking of underactuated UUVs. Accordingly, the output feedback spatial trajectory tracking problem of underactuated UUVs is extremely valuable and challenging.

Sliding mode control principle is a famous efficient nonlinear control theory to deal with control problems under parameter perturbation, bounded uncertainty/disturbances and parasitic dynamics of nonlinear system [40], [41]. Accordingly, the SMC is widely applied to develop the controllers of many nonlinear systems in recent decades, in view of the strong robustness, decoupling, fast response, and good dynamic characteristics of SMC [41], [42]. After more than half a century of development, the traditional SMC algorithm has evolved into a series of robust nonlinear control methods, including terminal SMC (TSMC), nonsingular terminal SMC (NTSMC), fast terminal SMC (FTSMC), proportional-integral-derivative SMC (PID-SMC) and so on [43]–[46]. In recent decades, SMC-class algorithms have been employed to solve the full-state-feedback motion control problem of underactuated marine vehicles [4], [10], [20], [23]–[26], [42], [47], [48]. For the discussed earlier, however, the full-state feedback control strategies may be inappropriate in many practical applications because not all states of the marine vehicles are measurable. The output feedback controllers have been proposed based the SMC-class control and sliding mode observer (SMO) algorithms [37], [38], [49]–[53]. Zhao *et al.* [38] proposed a novel output feedback TSMC approach for a class of second order nonlinear systems by using TSMC and the equivalent output injection SMO. For the motion control problem of ROV, a multivariable output feedback adaptive NTSMC scheme was developed [21], [36]. However, these motion control strategies of ROV cannot be directly applied to solve the trajectory tracking problem of underactuated UUV.

In this work, an output feedback control strategy is proposed for the spatial trajectory tracking of underactuated UUVs with parameter perturbation and external disturbances by using the equivalent output injection SMO, backstepping and first-order integral SMC. The motion state observer with excellent robustness against parameter perturbation can reconstruct the linear and angular velocities of underactuated UUVs in finite time, which is developed to adopt the equivalent output injection SMO. Then, the tracking controller of underactuated UUVs is designed based on the bioinspired filtering backstepping and first-order integral SMC, which can drive it to the desired trajectory and stabilize all tracking errors to the bounded neighborhood of the origin.

The remainder of this article is organized as follows. Section II describes the motion model of underactuated UUV and problem formulation. In section III, the output feedback spatial trajectory tracking control scheme for underactuated UUVs is presented. In section IV, numerical simulations are performed to validate the effectiveness of the proposed tracking control scheme. Finally, brief conclusions are drawn in section V.

II. PROBLEM FORMULATION

A. UUV KINEMATICS AND DYNAMICS

In this work, the type of underactuated UUVs is equipped with three independent motion control actuators, including a pair of the identical stern thrusters, a pair of sternplanes and a pair of rudders which are mounted symmetrically in the aft. For an underactuated UUV, its motion is six degrees of freedom (6-DOF) in the three-dimensional undersea space, described in the inertial reference frame $\{n\}$ and body-fixed reference frame $\{b\}$. In practical engineering, the roll motion of underactuated UUVs is usually neglected to simplify the design of the motion controller, because it is self-stabilized, small amounts compared to other degrees of freedom and not directly controlled by any motion control actuators. Therefore, the spatial motion for the type of underactuated UUVs can be described by the 5-DOF kinematic equations, as follows:

$$\begin{bmatrix} \dot{\boldsymbol{p}}^n_{b/n} \\ \dot{\boldsymbol{\Theta}}_{nb} \end{bmatrix} = \begin{bmatrix} \mathbf{R}^n_b(\boldsymbol{\Theta}_{nb}) & \mathbf{0}_{3\times3} \\ \mathbf{0}_{3\times3} & \mathbf{T}_\Theta(\boldsymbol{\Theta}_{nb}) \end{bmatrix} \begin{bmatrix} \boldsymbol{v}^b_{b/n} \\ \boldsymbol{\omega}^b_{b/n} \end{bmatrix} \tag{1}$$

where, the matrices $\mathbf{R}_b^n(\mathbf{\Theta}_{nb})$ and $\mathbf{T}_\Theta(\mathbf{\Theta}_{nb})$ are given by:

$$\mathbf{R}_b^n(\mathbf{\Theta}_{nb}) = \begin{bmatrix} \cos\psi\cos\theta & -\sin\psi & \cos\psi\sin\theta \\ \sin\psi\cos\theta & \cos\psi & \sin\psi\sin\theta \\ -\sin\theta & 0 & \cos\theta \end{bmatrix} \quad (2)$$

$$\mathbf{T}_\Theta(\mathbf{\Theta}_{nb}) = \begin{bmatrix} 1 & 0 \\ 0 & 1/\cos\theta \end{bmatrix} \quad (3)$$

where $\boldsymbol{p}_{b/n}^n = [x, y, z]^{\mathrm{T}}$ and $\mathbf{\Theta}_{nb} = [\theta, \psi]^{\mathrm{T}}$ denote the position and orientation of UUVs, respectively. Here, $\theta \in (-\pi/2, \pi/2)$ and $\psi \in (-\pi, \pi]$. Then, the position and orientation of an underactuated UUV are summed up $\boldsymbol{\eta} = [\boldsymbol{p}_{b/n}^{n\mathrm{T}}, \mathbf{\Theta}_{nb}^{\mathrm{T}}]^{\mathrm{T}}$. The symbols $\boldsymbol{v}_{b/n}^b = [u, v, w]^{\mathrm{T}}$ and $\boldsymbol{\omega}_{b/n}^b = [q, r]^{\mathrm{T}}$ represent the linear and angular velocities in $\{b\}$, and they are summed up $\boldsymbol{\nu} = [\boldsymbol{v}_{b/n}^{b\mathrm{T}}, \boldsymbol{\omega}_{b/n}^{b\mathrm{T}}]^{\mathrm{T}}$.

In practical engineering, the hull of UUVs can be a neutrally buoyant rigid body that its mass distribution is homogeneous. Meanwhile, in order to facilitate the analysis and design of motion control for underactuated UUVs, the order of the hydrodynamic drag terms is lower than two in the dynamic equations. According to the above assumption, the kinetic equations for a neutrally buoyant underactuated UUV with three planes of symmetry are simplified as follows

$$\begin{cases} m_{11}\dot{u} = m_{22}vr - m_{33}wq - X_u u - X_{u|u|}u\,|u| + \tau_1 \\ m_{22}\dot{v} = -m_{11}ur - Y_v v - Y_{v|v|}v\,|v| \\ m_{33}\dot{w} = m_{11}uq - Z_w w - Z_{w|w|}w\,|w| \\ m_{55}\dot{q} = (m_{33} - m_{11})uw - M_q q - M_{q|q|}q\,|q| \\ \qquad -(z_G W - z_B B)\sin\theta + \tau_5 \\ m_{66}\dot{r} = (m_{11} - m_{22})uv - N_r r - N_{r|r|}r\,|r| + \tau_6 \end{cases} \quad (4)$$

where τ_1, τ_5 and τ_6 denote the forward force, pitch torque and yaw torque, respectively. The constants m_{ii} $(i = 1, 2, 3, 5, 6)$ are the inertia including added mass effects. X_u, Y_v, Z_w, M_q and N_r are hydro-dynamic coefficients of the linear drag terms. $X_{u|u|}$, $Y_{v|v|}$, $Z_{w|w|}$, $M_{q|q|}$ and $N_{r|r|}$ indicate hydrodynamic coefficients of the quadratic drag terms. The insignias z_G and z_B represent the z_b-coordinate component of the center of gravity and the CB in the body-fixed coordinate frame $\{b\}$, respectively; W and B are gravity and buoyancy of the vehicle, respectively. In this work, the parameter perturbation is considered, i.e., there are $\pm 20\%$ uncertainties in the hydrodynamic coefficients of this underactuated UUV. The nominal values of rigid body and hydrodynamic coefficients for this underactuated UUV are given as [54].

B. CONTROL OBJECTIVES

For a practical UUV, the desired reference trajectory $\boldsymbol{p}_{\mathrm{R}}^n(t) = [x_{\mathrm{R}}, y_{\mathrm{R}}, z_{\mathrm{R}}]^{\mathrm{T}}$ must be a sufficiently smooth vector-function of time in the three-dimensional underwater space. Considering that the motion of the underactuated UUV is constrained by its own characteristics (including mechanical properties and security constraints), the desired reference trajectory $\boldsymbol{p}_{\mathrm{R}}^n(t)$ must satisfy the following geometric conditions:

$$K_{\mathrm{R}} = \frac{|\dot{x}_{\mathrm{R}}\ddot{y}_{\mathrm{R}} - \ddot{x}_{\mathrm{R}}\dot{y}_{\mathrm{R}}|}{(\dot{x}_{\mathrm{R}}^2 + \dot{y}_{\mathrm{R}}^2)^{3/2}} \le \frac{1}{\xi_{\mathrm{m}}}, \quad \frac{|\dot{z}_{\mathrm{R}}|}{\sqrt{\dot{x}_{\mathrm{R}}^2 + \dot{y}_{\mathrm{R}}^2}} \le \tan\theta_{\max} \quad (5)$$

where ξ_{m} and $\theta_{\max}$ denote the minimum turning radius and maximum pitch angle of this underactuated UUV respectively, K_{R} is the curvature of the desired reference trajectory $\boldsymbol{p}_{\mathrm{R}}^n(t)$, and the variables $\dot{x}_{\mathrm{R}}$, $\ddot{x}_{\mathrm{R}}$, $\dot{y}_{\mathrm{R}}$, $\ddot{y}_{\mathrm{R}}$ and $\dot{z}_{\mathrm{R}}$ are he first- and second-order time-derivatives of the position coordinate component x_{R}, y_{R} and z_{R}, respectively.

Under the designed spatial trajectory tracking control strategy, the motion states $\boldsymbol{p}_{b/n}^n(t)$, $\mathbf{\Theta}_{nb}(t)$, $\boldsymbol{v}_{b/n}^b(t)$ and $\boldsymbol{\omega}_{b/n}^b(t)$ of this underactuated UUV can converge to their respective desired value $\boldsymbol{p}_{\mathrm{R}}^n(t)$, $\mathbf{\Theta}_{\mathrm{R}}(t)$, $\boldsymbol{v}_{\mathrm{R}}(t)$ and $\boldsymbol{\omega}_{\mathrm{R}}(t)$, i.e.

$$\lim_{t\to\infty}(\boldsymbol{p}_{b/n}^n(t) - \boldsymbol{p}_{\mathrm{R}}^n(t)) = \mathbf{0}, \quad \lim_{t\to\infty}(\mathbf{\Theta}_{nb}(t) - \mathbf{\Theta}_{\mathrm{R}}(t)) = \mathbf{0} \quad (6)$$

$$\lim_{t\to\infty}(\boldsymbol{v}_{b/n}^b(t) - \boldsymbol{v}_{\mathrm{R}}(t)) = \mathbf{0}, \quad \lim_{t\to\infty}(\boldsymbol{\omega}_{b/n}^b(t) - \boldsymbol{\omega}_{\mathrm{R}}(t)) = \mathbf{0} \quad (7)$$

At the same time, all other motion states of this underactuated UUV are kept bounded for any initial conditions $\boldsymbol{p}_{b/n}^n(t_0)$, $\mathbf{\Theta}_{nb}(t_0)$, $\boldsymbol{v}_{b/n}^b(t_0)$ and $\boldsymbol{\omega}_{b/n}^b(t_0)$.

III. OUTPUT FEEDBACK TRAJECTORY TRACKING CONTROL STRATEGY

The design procedure of spatial trajectory tracking control is composed of three parts, including the tracking error equation construction, the motion-state observer design and the output feedback trajectory tracking controller design. First, the spatial trajectory tracking error dynamic equations are derived for the tracking controller design. Then, the motion state observer is developed to employ the equivalent output injection SMO, to reconstruct the motion states of an underactuated UUV. Finally, the output feedback trajectory tracking control scheme is proposed, involving the bio-inspired filtered backstepping, integral SMC and the motion-state sliding mode observer, to achieve the spatial trajectory tracking tasks of underactuated UUVs.

A. TRACKING ERROR EQUATIONS

For the spatial trajectory tracking of underactuated UUVs, the primary task is how to steer the position and attitude of underactuated UUVs to track the desired reference trajectory $\boldsymbol{p}_{b/n}^n(t)$. The following tracking position error variables $\boldsymbol{p}_e^n$ in $\{n\}$ are defined as

$$\boldsymbol{p}_e^n = \boldsymbol{p}_{b/n}^n - \boldsymbol{p}_{\mathrm{R}}^n \quad (8)$$

Then, using the coordinate transformation matrix(2), the tracking position error variables $\boldsymbol{p}_e^b$ in $\{b\}$ are written as

$$\boldsymbol{p}_e^b = \mathbf{R}_b^n(\mathbf{\Theta}_{nb})^{-1}\boldsymbol{p}_e^n \quad (9)$$

Because the coordinate transformation (9) is orthogonal, the tracking position error variables in $\{n\}$ and $\{b\}$ are equivalent to each other, namely $\boldsymbol{p}_e^b = [0, 0, 0]^{\mathrm{T}} \Leftrightarrow \boldsymbol{p}_e^n = [0, 0, 0]^{\mathrm{T}}$. That is to say, the stabilization of the tracking errors (8) and (9) are equivalent to each other.

Since the surge velocity of underactuated UUVs is much larger than its own sway and heave velocity, its sideslip angle and angle of attack can be considered approximately equal

to zero. Thus, the desired pitch and yaw angle of underactuated UUVs are calculated as

$$\theta_{\mathrm{R}} = -\arctan\frac{\dot{z}_{\mathrm{R}}}{\sqrt{\dot{x}_{\mathrm{R}}^2+\dot{y}_{\mathrm{R}}^2}}, \quad \psi_{\mathrm{R}} = \arctan\frac{\dot{y}_{\mathrm{R}}}{\dot{x}_{\mathrm{R}}} \tag{10}$$

The tracking attitude errors are defined as

$$\theta_e = \theta - \theta_{\mathrm{R}}, \quad \psi_e = \psi - \psi_{\mathrm{R}} \tag{11}$$

Calculating the derivative of the tracking error transformation Eq. (9) and substituting into the kinematic Eq. (1), the dynamic equations of the tracking position errors are obtained as follows:

$$\begin{cases} \dot{x}_e = u - u_{\mathrm{R}}(\cos\psi_e\cos\theta\cos\theta_{\mathrm{R}} + \sin\theta\sin\theta_{\mathrm{R}}) \\ \qquad +ry_e - qz_e \\ \dot{y}_e = v + u_{\mathrm{R}}\sin\psi_e\cos\theta_{\mathrm{R}} - r(x_e + z_e\tan\theta) \\ \dot{z}_e = w - u_{\mathrm{R}}(\cos\psi_e\sin\theta\cos\theta_{\mathrm{R}} - \cos\theta\sin\theta_{\mathrm{R}}) \\ \qquad +qx_e + ry_e\tan\theta \end{cases} \tag{12}$$

where the notation u_{R} is the desired surge velocity of the underactuated UUV and equals $\sqrt{\dot{x}_{\mathrm{R}}^2+\dot{y}_{\mathrm{R}}^2+\dot{z}_{\mathrm{R}}^2}$. Since the underactuated UUVs lack the direct control inputs in the sway and heave DOF, the desired sway and heave velocities equal zero, that is, $v_{\mathrm{R}} = 0$ and $w_{\mathrm{R}} = 0$. Next, tacking the derivatives of the tracking attitude errors, the dynamic equations of the tracking attitude error variables are calculated as follows:

$$\begin{cases} \dot{\theta}_e = q - q_{\mathrm{R}} \\ \dot{\psi}_e = r/\cos\theta - r_{\mathrm{R}}/\cos\theta_{\mathrm{R}} \end{cases} \tag{13}$$

where q_{R} and r_{R} indicate the desired pitch and yaw angular velocities, and their specific expressions are

$$\begin{cases} q_{\mathrm{R}} = \dot{\theta}_{\mathrm{R}} = (\dot{z}_{\mathrm{R}}\dot{\nu}_{\mathrm{t}} - \ddot{z}_{\mathrm{R}}\nu_{\mathrm{t}})/u_{\mathrm{R}}^2 \\ r_{\mathrm{R}} = \dot{\psi}_{\mathrm{R}}\cos\theta_{\mathrm{R}} = (\ddot{y}_{\mathrm{R}}\dot{x}_{\mathrm{R}} - \dot{y}_{\mathrm{R}}\ddot{x}_{\mathrm{R}})/\nu_{\mathrm{t}}u_{\mathrm{R}} \end{cases} \tag{14}$$

where the auxiliary variable ν_{t} equals $\sqrt{\dot{x}_{\mathrm{R}}^2+\dot{y}_{\mathrm{R}}^2}$.

B. THE MOTION-STATE OBSERVER

In this subsection, the motion-state observer is designed based on the equivalent output injection SMO, which can reconstruct the motion state of underactuated UUVs in finite time. To facilitate the design procedure of the motion-stare observer, the motion model of underactuated UUVs is rewritten as vector form in the inertial reference frame $\{n\}$. The rewritten motion model is expressed as

$$\begin{cases} \dot{\boldsymbol{x}}_1 = \boldsymbol{x}_2 \\ \hat{\boldsymbol{M}}_n(\boldsymbol{x}_1)\dot{\boldsymbol{x}}_2 = -\hat{\boldsymbol{C}}_n(\boldsymbol{x}_1,\boldsymbol{x}_2)\boldsymbol{x}_2 - \hat{\boldsymbol{D}}_n(\boldsymbol{x}_1,\boldsymbol{x}_2)\boldsymbol{x}_2 \\ \qquad\qquad -\boldsymbol{g}_n(\boldsymbol{x}_1) + \boldsymbol{\tau}_n \end{cases} \tag{15}$$

where, $\boldsymbol{x}_1 = \boldsymbol{\eta}$ and $\boldsymbol{x}_2 = \boldsymbol{J}(\boldsymbol{\eta})\boldsymbol{v}$ denote pose (including the position and orientation) and generalized velocity in $\{n\}$. The parameter matrixes in Eq. (15) can be described as

$$\begin{aligned} \hat{\boldsymbol{M}}_n(\boldsymbol{x}_1) &= \boldsymbol{J}(\boldsymbol{\eta})\hat{\boldsymbol{M}}\boldsymbol{J}^{-1}(\boldsymbol{\eta}); \\ \hat{\boldsymbol{C}}_n(\boldsymbol{x}_1,\boldsymbol{x}_2) &= (\hat{\boldsymbol{C}}(\boldsymbol{J}^{-1}(\boldsymbol{\eta})\boldsymbol{x}_2) - \hat{\boldsymbol{M}}\boldsymbol{J}^{-1}(\boldsymbol{\eta})\dot{\boldsymbol{J}}(\boldsymbol{\eta}))\boldsymbol{J}^{-1}(\boldsymbol{\eta}); \\ \hat{\boldsymbol{D}}_I(\boldsymbol{x}_1,\boldsymbol{x}_2) &= \boldsymbol{J}(\boldsymbol{\eta})\hat{\boldsymbol{D}}(\boldsymbol{J}^{-1}(\boldsymbol{\eta})\boldsymbol{x_2})\boldsymbol{J}^{-1}(\boldsymbol{\eta}); \\ \boldsymbol{g}_n(\boldsymbol{\eta}) &= \boldsymbol{J}(\boldsymbol{\eta})\boldsymbol{g}(\boldsymbol{\eta}); \\ \boldsymbol{\tau}_I &= \boldsymbol{J}(\boldsymbol{\eta})\boldsymbol{\tau}. \end{aligned}$$

The transformation matrix $J(\eta)$ is defined as

$$\boldsymbol{J}(\boldsymbol{\eta}) = \begin{bmatrix} \mathbf{R}_b^n(\boldsymbol{\Theta}_{nb}) & \mathbf{0}_{3\times3} \\ \mathbf{0}_{3\times3} & \mathbf{T}_\Theta(\boldsymbol{\Theta}_{nb}) \end{bmatrix} \tag{16}$$

And, the matrix $\hat{\boldsymbol{M}}, \hat{\boldsymbol{C}}(\boldsymbol{v}), \hat{\boldsymbol{D}}(\boldsymbol{v}), \boldsymbol{g}(\boldsymbol{\eta})$ and $\boldsymbol{\tau}$ are

$$\begin{aligned} \hat{\boldsymbol{M}} &= \mathrm{diag}(\hat{m}_{11}, \hat{m}_{22}, \hat{m}_{33}, \hat{m}_{55}, \hat{m}_{66}) \\ \hat{\boldsymbol{C}}(\boldsymbol{v}) &= -\hat{\boldsymbol{C}}^{\mathrm{T}}(\boldsymbol{v}) = \begin{bmatrix} 0 & -mr & mq & -\hat{Z}_{\dot{w}}w & \hat{Y}_{\dot{v}}v \\ mr & 0 & 0 & 0 & -\hat{X}_{\dot{u}}u \\ -mq & 0 & 0 & \hat{X}_{\dot{u}}u & 0 \\ \hat{Z}_{\dot{w}}w & 0 & -\hat{X}_{\dot{u}}u & 0 & 0 \\ -\hat{Y}_{\dot{v}}v & \hat{X}_{\dot{u}}u & 0 & 0 & 0 \end{bmatrix} \\ \hat{\boldsymbol{D}}(\boldsymbol{v}) &= diag(\hat{X}_u, \hat{Y}_v, \hat{Z}_w, \hat{M}_q, \hat{N}_r) \\ &\quad + diag(\hat{X}_{u|u|}\,|u|\,, \hat{Y}_{v|v|}\,|v|\,, \hat{Z}_{w|w|}\,|w|\,, \\ &\quad \times \hat{M}_{q|q|}\,|q|\,, \hat{N}_{r|r|}\,|r|) \\ \boldsymbol{g}(\boldsymbol{\eta}) &= [0, 0, 0, \overline{BG}_z W\sin\theta, 0]^{\mathrm{T}} \\ \boldsymbol{\tau} &= [\tau_1, 0, 0, \tau_5, \tau_6]^{\mathrm{T}} \end{aligned}$$

The motion state x_1 in Eq. (15) is measurable state variables, that is, the measured outputs of the system(15). The motion state x_2 is unmeasurable and need to be estimated by the motion state observer. The design procedure of the motion state observer is organized as follows:

Theorem 1: Consider the motion model (15) of underactuated UUVs with parameter perturbation. The motion state observer

$$\begin{cases} \dot{\hat{\boldsymbol{x}}}_1 = \hat{\boldsymbol{x}}_2 + \boldsymbol{\gamma}_1\mathrm{sgn}(\boldsymbol{x}_1 - \hat{\boldsymbol{x}}_1) \\ \hat{\boldsymbol{M}}_n(\boldsymbol{x}_1)\dot{\hat{\boldsymbol{x}}}_2 = -\hat{\boldsymbol{C}}_n(\boldsymbol{x}_1,\hat{\boldsymbol{x}}_2)\hat{\boldsymbol{x}}_2 - \hat{\boldsymbol{D}}_n(\boldsymbol{x}_1,\hat{\boldsymbol{x}}_2)\hat{\boldsymbol{x}}_2 \\ \qquad\qquad -\boldsymbol{g}_n(\boldsymbol{x}_1) + \boldsymbol{\tau}_n + \hat{\boldsymbol{\gamma}}_2\mathrm{sgn}(\bar{\boldsymbol{x}}_2 - \hat{\boldsymbol{x}}_2) \end{cases} \tag{17}$$

can reconstruct the motion states of this underactuated UUV, and can ensure that the estimation error $\tilde{\boldsymbol{x}}_1$ converges to the origin in a finite time and the estimation error $\tilde{\boldsymbol{x}}_2$ converges to a neighborhood of the origin in a finite time.

Remark 1: $\hat{\boldsymbol{x}}_1$ and $\hat{\boldsymbol{x}}_2$ are the estimated values of the motion states $\boldsymbol{x}_1$ and $\boldsymbol{x}_2$, respectively. The estimated errors $\tilde{\boldsymbol{x}}_1$ and $\tilde{\boldsymbol{x}}_2$ are $\tilde{\boldsymbol{x}}_1 = \boldsymbol{x}_1 - \hat{\boldsymbol{x}}_1$ and $\tilde{\boldsymbol{x}}_2 = \boldsymbol{x}_2 - \hat{\boldsymbol{x}}_2$. $\boldsymbol{\gamma}_1 = \mathrm{diag}(\gamma_{11}, \gamma_{12}, \gamma_{13}, \gamma_{15}, \gamma_{16})$ with $\gamma_{1i} > 0$ ($i = 1, 2, 3, 5, 6$) is the gain coefficient matrix of the motion state observer. $\bar{\boldsymbol{x}}_2 = \hat{\boldsymbol{x}}_2 + (\boldsymbol{\gamma}_1\mathrm{sgn}(\tilde{\boldsymbol{x}}_1))_{bo}$, and $(\boldsymbol{\gamma}_1\mathrm{sgn}(\tilde{\boldsymbol{x}}_1))_{bo}$ is the equivalent output injection, which can be obtained by passing the signal $\boldsymbol{\gamma}_1\mathrm{sgn}(\tilde{\boldsymbol{x}}_1)$ through a low pass filter [21]. $\hat{\boldsymbol{\gamma}}_2 = \mathrm{diag}(\hat{\gamma}_{21}, \hat{\gamma}_{22}, \hat{\gamma}_{23}, \hat{\gamma}_{25}, \hat{\gamma}_{26})$ is the adaptive gain coefficient matrix of the state observer, and $\dot{\hat{\gamma}}_{2i} = -\varepsilon_{0i}\hat{\gamma}_{2i} + \varepsilon_{1i}\left|\bar{x}_{2i} - \hat{x}_{2i}\right|$ ($\varepsilon_{0i} > 0$ and $\varepsilon_{1i} > 0$, $i = 1, 2, 3, 5, 6$).

Proof: The proof is composed of two steps. To analyze the convergence of the estimated errors $\tilde{\boldsymbol{x}}_1$ and $\tilde{\boldsymbol{x}}_2$ for the motion state observer (17), the dynamic equations of the estimated errors $\tilde{\boldsymbol{x}}_1$ and $\tilde{\boldsymbol{x}}_2$ are developed by subtracting Eq. (15)

from Eq. (17).

$$\begin{cases} \dot{\tilde{\boldsymbol{x}}}_1 = \tilde{\boldsymbol{x}}_2 - \boldsymbol{\gamma}_1 \mathrm{sgn}(\boldsymbol{x}_1 - \hat{\boldsymbol{x}}_1) \\ \dot{\tilde{\boldsymbol{x}}}_2 = \hat{\boldsymbol{M}}_n(\boldsymbol{x}_1)^{-1}(\boldsymbol{\delta}(\boldsymbol{x}_1, \boldsymbol{x}_2, \hat{\boldsymbol{x}}_2) - \hat{\boldsymbol{\gamma}}_2 \mathrm{sgn}(\bar{\boldsymbol{x}}_2 - \hat{\boldsymbol{x}}_2)) \end{cases} \tag{18}$$

where, $\boldsymbol{\delta}(\boldsymbol{x}_1, \boldsymbol{x}_2, \hat{\boldsymbol{x}}_2) = \hat{\boldsymbol{C}}_n(\boldsymbol{x}_1, \hat{\boldsymbol{x}}_2)\hat{\boldsymbol{x}}_2 - \hat{\boldsymbol{C}}_n(\boldsymbol{x}_1, \boldsymbol{x}_2)\boldsymbol{x}_2 + \hat{\boldsymbol{D}}_n(\boldsymbol{x}_1, \hat{\boldsymbol{x}}_2)\hat{\boldsymbol{x}}_2 - \hat{\boldsymbol{D}}_n(\boldsymbol{x}_1, \boldsymbol{x}_2)\boldsymbol{x}_2$.

Step1: To analyze the convergence of the estimated errors $\tilde{\boldsymbol{x}}_1$, the following Lyapunov function is chosen as

$$V_{o1} = \frac{1}{2}\tilde{\boldsymbol{x}}_1^{\mathrm{T}}\tilde{\boldsymbol{x}}_1 \tag{19}$$

The derivative of the Lyapunov function (19) is calculated according to the first formula of Eq.(18):

$$\dot{V}_{o1} = \tilde{\boldsymbol{x}}_1^{\mathrm{T}}\dot{\tilde{\boldsymbol{x}}}_1 = \tilde{\boldsymbol{x}}_1^{\mathrm{T}}(\tilde{\boldsymbol{x}}_2 - \boldsymbol{\gamma}_1 \mathrm{sgn}(\tilde{\boldsymbol{x}}_1)) = -\sum_{i \in S}(\gamma_{1i} - |\tilde{x}_{2i}|)\,|\tilde{x}_{1i}|$$

with $S = \{1, 2, 3, 5, 6\}$. The motion equations (15) of underactuated UUVs does not exist the finite escape time and the control inputs $\boldsymbol{\tau}_n$ belong to the extended L_p space, that is, the cutoff values in any finite-time are bounded. Therefore, the observer errors $\tilde{\boldsymbol{x}}_1$ do not exist the finite escape time and belong the extended L_p space. Then, the observer gain coefficient $\gamma_{1i}(i = 1, 2, 3, 5, 6)$ are selected to satisfy the following conditions $\gamma_{1i} > |\tilde{x}_{2i}| + \sigma_{1i}$ $(\sigma_{1i} > 0)$, so that the derivative $\dot{V}_{o1}$ of the Lyapunov function can satisfy the following inequality:

$$\begin{aligned} \dot{V}_{o1} &\le -\sum_{i \in S}\sigma_{1i}\,|\tilde{x}_{1i}| \le -\min_{i \in S}(\sigma_{1i})\sum_{i \in S}|\tilde{x}_{1i}| \\ &\le -\sqrt{2}\min_{i \in S}(\sigma_{1i})V_{o1}^{\frac{1}{2}} \end{aligned} \tag{20}$$

According to Lemma 1 in [10], the observer error $\tilde{\boldsymbol{x}}_1$ can converge to the equilibrium point in finite time, and the convergence time of the observer error $\tilde{x}_{1i}$ meet the following conditions respectively:

$$t_{1i} \le t_0 + \frac{|\tilde{x}_{1i}|}{\sigma_{1i}}, \quad i \in S \tag{21}$$

where t_0 is the initial time. When $t \ge t_{1i}$, the observer error $\tilde{\boldsymbol{x}}_1$ and their derivative are all zero. Then, $\tilde{\boldsymbol{x}}_1$, $\dot{\tilde{\boldsymbol{x}}}_1$ and $\tilde{\boldsymbol{x}}_2 = (\boldsymbol{\gamma}_1 \mathrm{sgn}(\tilde{\boldsymbol{x}}_1))_{bo}$ are on the sliding surface. Thus, the dynamic equations (18) of the estimated errors become

$$\begin{cases} \dot{\tilde{\boldsymbol{x}}}_1 = \boldsymbol{0} \\ \dot{\tilde{\boldsymbol{x}}}_2 = \hat{\boldsymbol{M}}_I(\boldsymbol{x}_1)^{-1}(\boldsymbol{\delta}(\boldsymbol{x}_1, \boldsymbol{x}_2, \hat{\boldsymbol{x}}_2) + \boldsymbol{\tau}_I^{\mathrm{d}} - \hat{\boldsymbol{\gamma}}_2 \mathrm{sgn}(\bar{\boldsymbol{x}}_2 - \hat{\boldsymbol{x}}_2)) \end{cases} \tag{22}$$

Step2: Next, the convergence of the state estimation error $\tilde{x}_2$ is analyzed. Consider the following Lyapunov functions:

$$V_{o2} = V_{o1} + \frac{1}{2}\tilde{\boldsymbol{x}}_2^{\mathrm{T}}\hat{\boldsymbol{M}}_I(\boldsymbol{x}_1)\tilde{\boldsymbol{x}}_2 + \frac{1}{2}\sum_{i \in S}\tilde{\gamma}_{2i}^2 \tag{23}$$

where $\tilde{\gamma}_{2i} = \gamma_{2i} - \hat{\gamma}_{2i}$, and γ_{2i} are constants greater than zero. When $t \ge t_{1i}$, the derivative of the Lyapunov function (23) is calculated according to the second formula of Eq.(18):

$$\begin{aligned} \dot{V}_{o2} &= \tilde{\boldsymbol{x}}_2^{\mathrm{T}}\hat{\boldsymbol{M}}_I(\boldsymbol{x}_1)\dot{\tilde{\boldsymbol{x}}}_2 + \sum_{i \in S}\tilde{\gamma}_{2i}\dot{\tilde{\gamma}}_{2i} \\ &= \tilde{\boldsymbol{x}}_2^{\mathrm{T}}(\boldsymbol{\delta}(\boldsymbol{x}_1, \boldsymbol{x}_2, \hat{\boldsymbol{x}}_2) + \boldsymbol{\tau}_I^{\mathrm{d}} - \hat{\boldsymbol{\gamma}}_2 \mathrm{sgn}(\bar{\boldsymbol{x}}_2 - \hat{\boldsymbol{x}}_2)) \\ &\quad - \sum_{i \in S}\tilde{\gamma}_{2i}(-\varepsilon_{0i}\hat{\gamma}_{2i} + \varepsilon_{1i}\left|\bar{x}_{2i} - \hat{x}_{2i}\right|) \\ &\le -\sum_{i \in S}|\tilde{x}_{2i}|\,(\hat{\gamma}_{2i} + \varepsilon_{1i}\tilde{\gamma}_{2i} - \left|\boldsymbol{\delta}(\boldsymbol{x}_1, \boldsymbol{x}_2, \hat{\boldsymbol{x}}_2) + \boldsymbol{\tau}_I^{\mathrm{d}}\right|_i) \\ &\quad + \sum_{i \in S}\varepsilon_{0i}\tilde{\gamma}_{2i}\hat{\gamma}_{2i} \end{aligned} \tag{24}$$

Then, by selecting the appropriate $\hat{\gamma}_{2i} \ge -\varepsilon_{1i}\tilde{\gamma}_{2i} + \left|\boldsymbol{\delta}(\boldsymbol{x}_1, \boldsymbol{x}_2, \hat{\boldsymbol{x}}_2)\right|_i + \sigma_{2i}$ $(\sigma_{2i} > 0)$, it is obtained as follows:

$$\begin{aligned} \dot{V}_{o2} &\le \sum_{i \in S}(-\sigma_{2i}\,|\tilde{x}_{2i}| + \varepsilon_{0i}\tilde{\gamma}_{2i}\hat{\gamma}_{2i}) \\ &= \sum_{i \in S}(-\sqrt{\frac{2\sigma_{2i}^2}{\hat{m}_{ii}}}(\frac{1}{2}\hat{m}_{ii}\tilde{x}_{2i}^2)^{\frac{1}{2}} - \sqrt{\frac{2\sigma_{2i}^2}{\hat{m}_{ii}}}(\frac{1}{2}\tilde{x}_{1i}^2)^{\frac{1}{2}} \\ &\quad - \sqrt{\frac{2\sigma_{2i}^2}{\hat{m}_{ii}}}(\frac{1}{2}\tilde{\gamma}_{2i}^2)^{\frac{1}{2}} + \sqrt{\frac{2\sigma_{2i}^2}{\hat{m}_{ii}}}(\frac{1}{2}\tilde{\gamma}_{2i}^2)^{\frac{1}{2}} + \varepsilon_{0i}\tilde{\gamma}_{2i}\hat{\gamma}_{2i}) \\ &\le -\sum_{i \in S}\sqrt{\frac{2\sigma_{2i}^2}{\hat{m}_{ii}}}V_{o2}^{\frac{1}{2}} + \sum_{i \in S}(\sqrt{\frac{\sigma_{2i}^2}{\hat{m}_{ii}}}\,|\tilde{\gamma}_{2i}| + \varepsilon_{0i}\tilde{\gamma}_{2i}\hat{\gamma}_{2i}) \end{aligned} \tag{25}$$

According to Lemma 2 in [21], when $|\tilde{\gamma}_{2i}| \ge 1$, the derivative of the Lyapunov function (23) satisfies:

$$\dot{V}_{o2} \le -\sum_{i \in S}\sqrt{\frac{2\sigma_{2i}^2}{\hat{m}_{ii}}}V_{o2}^{\frac{1}{2}} + \sum_{i \in S}\frac{\varepsilon_{0i}^2\sqrt{\hat{m}_{ii}}}{4(\varepsilon_{0i}\sqrt{\hat{m}_{ii}} - \sigma_{2i})}\gamma_{2i}^2 \tag{26}$$

Thus, according to Lemma 3 in [21], the state observer error $\tilde{\boldsymbol{x}}_2$ can converge to the neighborhood of an origin within a finite time, and the neighborhood of the origin is as follows:

$$\lim_{\theta \to \theta_0}\tilde{\boldsymbol{x}}_2 \in (V_{o2}^{\frac{1}{2}} \le \frac{\sum_{i \in S}\frac{\varepsilon_{0i}^2\hat{m}_{ii}}{2\sqrt{2}(\varepsilon_{0i}\sqrt{\hat{m}_{ii}} - \sigma_{2i})\sigma_{2i}}\gamma_{2i}^2}{(1-\theta)})$$

where $\theta_0 \in (0, 1)$. And the convergence time satisfies:

$$t_{2i} \le t_{1i} + \frac{\sqrt{2\hat{m}_{ii}}V_{o2}^{\frac{1}{2}}(\tilde{\boldsymbol{x}}_2)}{\sigma_{2i}\theta_0}$$

When $|\tilde{\gamma}_{2i}| < 1$, the derivative of the Lyapunov function (23) satisfies:

$$\dot{V}_{o2} \le -\sum_{i \in S}\sqrt{\frac{2\sigma_{2i}^2}{\hat{m}_{ii}}}V_{o2}^{\frac{1}{2}} + \sum_{i \in S}(\sqrt{\frac{\sigma_{2i}^2}{\hat{m}_{ii}}} + \varepsilon_{0i}\gamma_{2i}) \tag{27}$$

Then, according to Lemma 3 in [21], the state observer error $\tilde{\boldsymbol{x}}_2$ can converge to the neighborhood of an origin within a finite time. Thus, it is proved that regardless of the value of the observer adaptive gain error $\tilde{\gamma}_{2i}$, the state observer error $\tilde{\boldsymbol{x}}_2$ can converge to a neighborhood of the equilibrium point in a finite time. ■

Remark 2: To simplify design procedure of the output feedback tracking controller, the motion state observer (17) is converted from $\{n\}$ to $\{b\}$:

$$\begin{cases} \dot{\hat{\boldsymbol{\eta}}} = \boldsymbol{J}(\boldsymbol{\eta})\hat{\boldsymbol{v}} + \boldsymbol{\gamma}_1 \mathrm{sgn}(\tilde{\boldsymbol{\eta}}) \\ \hat{\boldsymbol{M}}\dot{\hat{\boldsymbol{v}}} = -\hat{\boldsymbol{C}}(\hat{\boldsymbol{v}})\hat{\boldsymbol{v}} - \hat{\boldsymbol{D}}(\hat{\boldsymbol{v}})\hat{\boldsymbol{v}} - \boldsymbol{g}(\boldsymbol{\eta}) + \boldsymbol{\tau} \\ +\boldsymbol{J}^{-1}(\boldsymbol{\eta})\hat{\boldsymbol{\gamma}}_2 \mathrm{sgn}(\boldsymbol{J}(\boldsymbol{\eta})\bar{\boldsymbol{v}} - \boldsymbol{J}(\boldsymbol{\eta})\hat{\boldsymbol{v}}) \end{cases} \tag{28}$$

where $\hat{\boldsymbol{\gamma}}_2 = \mathrm{diag}(\hat{\gamma}_{21}, \hat{\gamma}_{22}, \hat{\gamma}_{23}, \hat{\gamma}_{25}, \hat{\gamma}_{26})$ is the adaptive gain coefficient matrix of the state observer, and $\dot{\hat{\gamma}}_{2i} = -\varepsilon_{0i}\hat{\gamma}_{2i} + \varepsilon_{1i}\left|\boldsymbol{J}(\boldsymbol{\eta})\bar{\boldsymbol{v}} - \boldsymbol{J}(\boldsymbol{\eta})\hat{\boldsymbol{v}}\right|_i$ ($\varepsilon_{0i} > 0$ and $\varepsilon_{1i} > 0$, $i = 1, 2, 3, 5, 6$). $\boldsymbol{J}(\boldsymbol{\eta})\bar{\boldsymbol{v}} = \boldsymbol{J}(\boldsymbol{\eta})\hat{\boldsymbol{v}}_2 + (\boldsymbol{\gamma_1}\mathrm{sgn}(\tilde{\boldsymbol{\eta}}))_{eq}$, $\tilde{\boldsymbol{\eta}} = \boldsymbol{\eta} - \hat{\boldsymbol{\eta}}$.

Remark 3: From the motion state observer(28), the linear and angular velocities of underactuated UUVs can be obtained. To develop the tracking dynamic controller, the second equation of the motion state observer (28) is transformed into component form:

$$\begin{cases} \hat{m}_{11}\dot{\hat{u}} = \hat{m}_{22}\hat{v}\hat{r} - \hat{m}_{33}\hat{w}\hat{q} - \hat{X}_u\hat{u} - \hat{X}_{u|u|}\hat{u}\left|\hat{u}\right| + \tau_1 + f_{\hat{u}} \\ \hat{m}_{22}\dot{\hat{v}} = -\hat{m}_{11}\hat{u}\hat{r} - \hat{Y}_v\hat{v} - \hat{Y}_{v_{v|v|}}\hat{v}\left|\hat{v}\right| + f_{\hat{v}} \\ \hat{m}_{33}\dot{\hat{w}} = \hat{m}_{11}\hat{u}\hat{q} - \hat{Z}_w\hat{w} - \hat{Z}_{w|w|}\hat{w}\left|\hat{w}\right| + f_{\hat{w}} \\ \hat{m}_{55}\dot{\hat{q}} = (\hat{m}_{33} - \hat{m}_{11})\hat{u}\hat{w} - \hat{M}_q\hat{q} - \hat{M}_{q|q|}\hat{q}\left|\hat{q}\right| \\ \qquad -\overline{BG}_z W\sin\theta + \tau_5 + f_{\hat{q}} \\ \hat{m}_{66}\dot{\hat{r}} = (\hat{m}_{11} - \hat{m}_{22})\hat{u}\hat{v} - \hat{N}_r\hat{r} - \hat{N}_{r|r|}\hat{r}\left|\hat{r}\right| + \tau_6 + f_{\hat{r}} \end{cases} \tag{29}$$

where, $f_{\hat{u}}, f_{\hat{v}}, f_{\hat{w}}, f_{\hat{q}}$ and $f_{\hat{r}}$ are defined as

$$\begin{aligned} f_{\hat{u}} = {} & \hat{\gamma}_{21}\mathrm{sgn}((\bar{u} - \hat{u})\cos\psi\cos\theta - (\bar{v} - \hat{v})\sin\psi \\ & + (\bar{w} - \hat{w})\cos\psi\sin\theta)\cos\psi\cos\theta \\ & + \hat{\gamma}_{22}\mathrm{sgn}((\bar{u} - \hat{u})\sin\psi\cos\theta + (\bar{v} - \hat{v})\cos\psi \\ & + (\bar{w} - \hat{w})\sin\psi\sin\theta)\sin\psi\cos\theta \\ & - \hat{\gamma}_{23}\mathrm{sgn}(-(\bar{u} - \hat{u})\sin\theta + (\bar{w} - \hat{w})\cos\theta)\sin\theta \end{aligned}$$

$$\begin{aligned} f_{\hat{v}} = {} & -\hat{\gamma}_{21}\mathrm{sgn}((\bar{u} - \hat{u})\cos\psi\cos\theta - (\bar{v} - \hat{v})\sin\psi \\ & + (\bar{w} - \hat{w})\cos\psi\sin\theta)\sin\psi \\ & + \hat{\gamma}_{22}\mathrm{sgn}((\bar{u} - \hat{u})\sin\psi\cos\theta + (\bar{v} - \hat{v})\cos\psi \\ & + (\bar{w} - \hat{w})\sin\psi\sin\theta)\cos\psi \\ f_{\hat{w}} = {} & \hat{\gamma}_{21}\mathrm{sgn}((\bar{u} - \hat{u})\cos\psi\cos\theta - (\bar{v} - \hat{v})\sin\psi \\ & + (\bar{w} - \hat{w})\cos\psi\sin\theta)\cos\psi\sin\theta \\ & + \hat{\gamma}_{22}\mathrm{sgn}((\bar{u} - \hat{u})\sin\psi\cos\theta + (\bar{v} - \hat{v})\cos\psi \\ & + (\bar{w} - \hat{w})\sin\psi\sin\theta)\sin\psi\sin\theta \\ & + \hat{\gamma}_{23}\mathrm{sgn}(-(\bar{u} - \hat{u})\sin\theta + (\bar{w} - \hat{w})\cos\theta)\cos\theta \\ f_{\hat{q}} = {} & \hat{\gamma}_{25}\mathrm{sgn}(\bar{q} - \hat{q}) \\ f_{\hat{r}} = {} & \hat{\gamma}_{26}\mathrm{sgn}((\bar{r} - \hat{r})/\cos\theta)\cos\theta \end{aligned}$$

C. CTHE OUTPUT FEEDBACK TRACKING CONTROLLOR

To achieve the spatial trajectory tracking of underactuated UUVs, the tracking errors x_e, y_e, z_e, θ_e and ψ_e should be stabilized. Therefore, the control Lyapunov function is set as:

$$V_{kin} = \frac{1}{2}x_e^2 + \frac{1}{2}y_e^2 + \frac{1}{2}z_e^2 + (1 - \cos\theta_e) + (1 - \cos\psi_e) \tag{30}$$

Tacking the time-derivative of (30) the solution of Eqs. (12) and (13), it is obtained as follows:

$$\begin{aligned} \dot{V}_{kin} = {} & (u - u_{\mathrm{R}}(\cos\psi_e\cos\theta\cos\theta_{\mathrm{R}} + \sin\theta\sin\theta_{\mathrm{R}}))x_e \\ & + (q - q_{\mathrm{R}} - u_{\mathrm{R}}z_e\cos\psi_e)\sin\theta_e \\ & + (r/\cos\theta - r_{\mathrm{R}}/\cos\theta_{\mathrm{R}} + u_{\mathrm{R}}y_e\cos\theta_{\mathrm{R}})\sin\psi_e \\ & + (u_{\mathrm{R}}(1 - \cos\psi_e)\cos\theta\sin\theta_{\mathrm{R}} + w)z_e + vy_e \end{aligned} \tag{31}$$

To ensure that Eq.(31) is negative, the surge velocity u, pitch angular velocity q and yaw angular velocity r are treated as the virtual control inputs of the kinematic subsystem, and they are set to

$$\begin{cases} \delta_u = u_{\mathrm{R}}(\cos\psi_e\cos\theta\cos\theta_{\mathrm{R}} + \sin\theta\sin\theta_{\mathrm{R}}) - k_x x_e \\ \delta_q = q_{\mathrm{R}} + u_{\mathrm{R}}z_e\cos\psi_e - k_\theta\sin\theta_e \\ \delta_r = (r_{\mathrm{R}}/\cos\theta_{\mathrm{R}} - u_{\mathrm{R}}y_e\cos\theta_{\mathrm{R}} - k_\psi\sin\psi_e)\cos\theta \end{cases} \tag{32}$$

where k_x, k_θ and k_ψ are the adjustment gain coefficients and all positive. To avoid complex differential calculations for the virtual controller(32), the bioinspired filter based the Shunting Neural Dynamics Model is introduced [55]–[57]. The Shunting Neural Dynamics Model is derived from Hodgkin's and Huxley's research concerning the ionic mechanisms related to the excitation and inhibition of the peripheral and central parts of nerve cell membranes [55], [56]. The dynamics of voltage across the membrane can be expressed by differential equations as follows:

$$C_m\frac{\mathrm{d}V_m}{\mathrm{d}t} = -(E_p + V_m)g_p + (E_{Na} - V_m)g_{Na} - (E_K + V_m)g_K \tag{33}$$

where V_m is the voltage across the membrane. The notation C_m is the membrane capacitance, and the parameters E_K, E_{Na} and E_p are the Nernst potentials for potassium ions, sodium ions, and passive leak current in the membrane, respectively. The symbols g_K, g_{Na} and g_p are the conductance of potassium and sodium, and the passive channels are functions of input signals that vary with time. Substituting $C_m = 1, x = E_p + V_m, A = g_p, B = E_{Na} + E_p, D = E_K - E_p$, $S^+ = g_{\mathrm{Na}}$ and $S^- = g_{\mathrm{K}}$ into Eq. (33), the Shunting Neural Dynamics Model can be obtained [55], [56]

$$\frac{\mathrm{d}x}{\mathrm{d}t} = -Ax + (B - x)S^+(t) - (D + x)S^-(t) \tag{34}$$

where, x is the neural activity (membrane potential) of the neuron. A, B and D are the passive decay rate, the upper and the lower bounds of the neural activity, respectively, and are all nonnegative constants. $S^+(t)$ and $S^-(t)$ are the excitatory and inhibitory inputs, respectively. The virtual controller (32) is set to the inputs of this bioinspired filter, that is,

$$\begin{cases} \dot{\delta}_u^* = -A_u\delta_u^* + (B_u - \delta_u^*)f(\delta_u) - (D_u + \delta_u^*)g(\delta_u) \\ \dot{\delta}_q^* = -A_q\delta_q^* + (B_q - \delta_q^*)f(\delta_q) - (D_q + \delta_q^*)g(\delta_q) \\ \dot{\delta}_r^* = -A_r\delta_r^* + (B_r - \delta_r^*)f(\delta_r) - (D_r + \delta_r^*)g(\delta_r) \end{cases} \tag{35}$$

where, $f(x) = \max(x, 0)$ denotes the excitatory; $g(x) = \max(-x, 0)$; δ_u^*, δ_q^*, δ_r^* are outputs of the bioinspired filter. This bioinspired filter is a continuous differential equation,

which guarantees that its output remains in a region $[-D, B]$ for any excitatory and inhibitory inputs. However, the tracking controllers (32) and (35) are not actual control inputs. Therefore, the tracking controller (32) or (35) does not achieve the trajectory tracking task of underactuated UUVs. To thoroughly implement the spatial trajectory tracking objectives, the dynamic tracking controller is developed to extend the virtual control law(35). Since the linear and angular velocities of underactuated UUV need to be estimated by the state observer(28), the following tracking error variables are introduced

$$\begin{cases} \hat{u}_e = \hat{u} - \delta_u^* \\ \hat{q}_e = \hat{q} - \delta_q^* \\ \hat{r}_e = \hat{r} - \delta_r^* \end{cases}, \quad \begin{cases} e_u = \delta_u^* - \delta_u \\ e_q = \delta_q^* - \delta_q \\ e_r = \delta_r^* - \delta_r \end{cases} \tag{36}$$

Further, substituting Eqs. (32) and (36) into Eq. (31), the derivative $\dot{V}_{kin}$ becomes

$$\begin{aligned} \dot{V}_{kin} = & -k_x x_e^2 - k_\theta \sin^2\theta_e - k_\psi \sin^2\psi_e \\ & + (u_e + e_u)x_e + (q_e + e_q)\sin\theta_e \\ & + ((r_e + e_r)\sin\psi_e)/\cos\theta \\ & + (u_{\mathrm{R}}(1 - \cos\psi_e)\cos\theta\sin\theta_{\mathrm{R}} + w)z_e + vy_e \end{aligned} \tag{37}$$

To ensure that Eq. (37) is negative, the dynamic tracking controller should be developed. Considering the parameter perturbation of underactuated UUVs, the dynamic equations of the tracking error variables $\hat{u}_e$, $\hat{q}_e$ and $\hat{r}_e$ can be obtained by tacking the derivatives of these tracking error variables and substituting the kinetic equations (4).

$$\begin{cases} \hat{m}_{11}\dot{\hat{u}}_e = \hat{m}_{22}\hat{v}\hat{r} - \hat{m}_{33}\hat{w}\hat{q} - \hat{X}_u\hat{u} - \hat{X}_{u|u|}\hat{u}\left|\hat{u}\right| - \hat{m}_{11}\dot{\delta}_u^* \\ \qquad +\tau_1 + f_{\hat{u}} + d_1^* \\ \hat{m}_{55}\dot{\hat{q}}_e = (\hat{m}_{33} - \hat{m}_{11})\hat{u}\hat{w} - \hat{M}_q\hat{q} - \hat{M}_{q|q|}\hat{q}\left|\hat{q}\right| \\ \qquad -\overline{BG}_z W\sin\theta - \hat{m}_{55}\dot{\delta}_q^* + \tau_5 + f_{\hat{q}} + d_5^* \\ \hat{m}_{66}\dot{\hat{r}}_e = (\hat{m}_{11} - \hat{m}_{22})\hat{u}\hat{v} - \hat{N}_r\hat{r} - \hat{N}_{r|r|}\hat{r}\left|\hat{r}\right| - \hat{m}_{66}\dot{\delta}_r^* \\ \qquad +\tau_6 + f_{\hat{r}} + d_6^* \end{cases} \tag{38}$$

where, $d_1^* = \tilde{m}_{11}\dot{u} - \tilde{m}_{11}\dot{\delta}_u^*$, $d_5^* = \tilde{m}_{55}\dot{q} - \tilde{m}_{55}\dot{\delta}_q^*$, $d_6^* = \tilde{m}_{66}\dot{r} - \tilde{m}_{66}\dot{\delta}_r^*$.

To thoroughly achieve the spatial trajectory tracking objectives, the following three integral terminal sliding surface are introduced

$$\begin{cases} S_u = \hat{u}_e + \lambda_u \int_0^t \mathrm{sig}^{\alpha_u}(\hat{u}_e(\tau))\mathrm{d}\tau \\ S_q = \hat{q}_e + \lambda_q \int_0^t \mathrm{sig}^{\alpha_q}(\hat{q}_e(\tau))\mathrm{d}\tau \\ S_r = \hat{r}_e + \lambda_r \int_0^t \mathrm{sig}^{\alpha_r}(\hat{r}_e(\tau))\mathrm{d}\tau \end{cases} \tag{39}$$

where λ_u, λ_q and λ_r are all positive constants representing integral coefficient of the integral terminal sliding surface. Parameters α_u, α_q and α_r are positive numbers belonging to $(1, 2)$. $sig^\alpha(x) = |x|^\alpha \mathrm{sgn}(x)$.

Calculating the derivative of sliding surface (39) yields

$$\begin{cases} \dot{S}_u = \dot{\hat{u}}_e + \lambda_u \mathrm{sig}^{\alpha_u}(\hat{u}_e) \\ \dot{S}_q = \dot{\hat{q}}_e + \lambda_q \mathrm{sig}^{\alpha_q}(\hat{q}_e) \\ \dot{S}_r = \dot{\hat{r}}_e + \lambda_r \mathrm{sig}^{\alpha_r}(\hat{r}_e) \end{cases} \tag{40}$$

Without considering parameter perturbation, the equivalent control law can be derived by solving $\dot{S}_u = 0$, $\dot{S}_q = 0$ and $\dot{S}_r = 0$ along the solution of Eq.(38).

$$\begin{cases} \tau_{1eq} = -\hat{m}_{22}\hat{v}\hat{r} + \hat{m}_{33}\hat{w}\hat{q} + \hat{X}_u\hat{u} + \hat{X}_{u|u|}\hat{u}\left|\hat{u}\right| \\ \qquad +\hat{m}_{11}\dot{\delta}_u^* - f_{\hat{u}} - \lambda_u\hat{m}_{11}\mathrm{sig}^{\alpha_u}(\hat{u}_e) \\ \tau_{5eq} = (\hat{m}_{11} - \hat{m}_{33})\hat{u}\hat{w} + \hat{M}_q\hat{q} + \hat{M}_{q|q|}\hat{q}\left|\hat{q}\right| \\ \qquad +\overline{BG}_z W\sin\theta + \hat{m}_{55}\dot{\delta}_q^* - f_{\hat{q}} - \lambda_q\hat{m}_{55}\mathrm{sig}^{\alpha_q}(\hat{q}_e) \\ \tau_{6eq} = (\hat{m}_{22} - \hat{m}_{11})\hat{u}\hat{v} + \hat{N}_r\hat{r} + \hat{N}_{r|r|}\hat{r}\left|\hat{r}\right| \\ \qquad +\hat{m}_{66}\dot{\delta}_r^* - f_{\hat{r}}\lambda_r - \hat{m}_{66}\mathrm{sig}^{\alpha_r}(\hat{r}_e) \end{cases} \tag{41}$$

However, the equivalent controllers cannot perform good trajectory tracking with parameter perturbation. Therefore, the reaching laws are introduced to this tracking control scheme, eliminating the effect of the parameter perturbation and disturbance.

$$\begin{cases} \tau_{1r} = -K_u\mathrm{sgn}(S_u) \\ \tau_{5r} = -K_q\mathrm{sgn}(S_q) \\ \tau_{6r} = -K_r\mathrm{sgn}(S_r) \end{cases} \tag{42}$$

where, K_u, K_q and K_r are the reaching law gains and specifically expressed as:

$$\begin{cases} K_u = \tilde{m}_{22}\left|\hat{v}\hat{r}\right| + \tilde{m}_{33}\left|\hat{w}\hat{q}\right| + \tilde{X}_u\left|\hat{u}\right| + \tilde{X}_{u|u|}\left|\hat{u}\right|^2 \\ \qquad +\tilde{m}_{11}\left|\dot{\delta}_u^*\right| + \lambda_u\tilde{m}_{11}\left|\hat{u}_e\right|^{\alpha_u} + \eta_u \\ K_q = (\tilde{m}_{11} + \hat{m}_{33})\left|\hat{u}\hat{w}\right| + \tilde{M}_q\left|\hat{q}\right| + \tilde{M}_{q|q|}\left|\hat{q}\right|^2 \\ \qquad +\tilde{m}_{55}\left|\dot{\delta}_q^*\right| + \lambda_q\tilde{m}_{55}\left|\hat{q}_e\right|^{\alpha_q} + \eta_q \\ K_r = (\tilde{m}_{11} + \tilde{m}_{22})\left|\hat{u}\hat{v}\right| + \tilde{N}_r\left|\hat{r}\right| + \tilde{N}_{r|r|}\left|\hat{r}\right|^2 \\ \qquad +\tilde{m}_{66}\left|\dot{\delta}_r^*\right| + \lambda_r\tilde{m}_{66}\left|\hat{r}_e\right|^{\alpha_r} + \eta_r \end{cases} \tag{43}$$

where, η_u, η_q and η_r are all positive constants to be determined. Then, the total state feedback tracking controller is as follows

$$\begin{cases} \tau_1 = \tau_{1eq} + \tau_{1r} = -\hat{m}_{22}\hat{v}\hat{r} + \hat{m}_{33}\hat{w}\hat{q} + \hat{X}_u\hat{u} + \hat{X}_{u|u|}\hat{u}\left|\hat{u}\right| \\ \qquad +\hat{m}_{11}\dot{\delta}_u^* - f_{\hat{u}} - \lambda_u\hat{m}_{11}\mathrm{sig}^{\alpha_u}(\hat{u}_e) - K_u\mathrm{sgn}(S_u) \\ \tau_5 = \tau_{5eq} + \tau_{5r} = (\hat{m}_{11} - \hat{m}_{33})\hat{u}\hat{w} + \hat{M}_q\hat{q} + \hat{M}_{q|q|}\hat{q}\left|\hat{q}\right| \\ \qquad +\overline{BG}_z W\sin\theta + \hat{m}_{55}\dot{\delta}_q^* - f_{\hat{q}} - \lambda_q\hat{m}_{55}\mathrm{sig}^{\alpha_q}(\hat{q}_e) \\ \qquad -K_q\mathrm{sgn}(S_q) \\ \tau_6 = \tau_{6eq} + \tau_{6r} = (\hat{m}_{22} - \hat{m}_{11})\hat{u}\hat{v} + \hat{N}_r\hat{r} + \hat{N}_{r|r|}\hat{r}\left|\hat{r}\right| \\ \qquad +\hat{m}_{66}\dot{\delta}_r^* - f_{\hat{r}} - \lambda_r\hat{m}_{66}\mathrm{sig}^{\alpha_r}(\hat{r}_e) - K_r\mathrm{sgn}(S_r) \end{cases} \tag{44}$$

The detailed block diagram of the output feedback spatial trajectory tracking control scheme is shown in Fig.1. Under the proposed trajectory tracking controller, the stability of the closed loop system for the trajectory tracking errors is organized as follows:

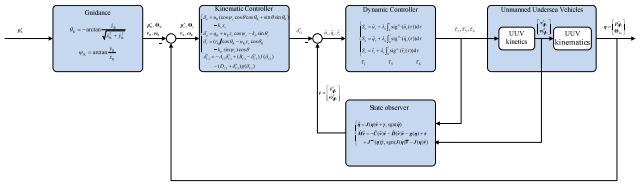

FIGURE 1. The block diagram of the output feedback spatial trajectory tracking controller.

Theorem 2: Consider the dynamic equations(12), (13) and (38) of the spatial trajectory tracking errors for underactuated UUVs with parameter perturbation and unmeasurable velocities. Under the output feedback spatial trajectory tracking control law (44), (32) and (35), the tracking error variables x_e, y_e, z_e, θ_e, ψ_e, $\hat{u}_e$, $\hat{q}_e$, $\hat{r}_e$, e_u, e_q and e_r are stabilized to the bounded neighborhood of the origin.

Proof: To analyze the stability of the closed-loop tracking control system, the control Lyapunov function are chosen as

$$V_{all} = \frac{1}{2}(m_{11}S_u^2 + m_{55}S_q^2 + m_{66}S_r^2) + \frac{1}{2}(e_u^2 + e_q^2 + e_r^2) + V_{kin} + V_{o2} \quad (45)$$

Tacking the derivative of the Lyapunov function (45) under the output feedback spatial trajectory tracking control law (44), (32) and (35), and substituting Eqs. (24) and (37),

$$\begin{aligned}\dot{V}_{all} =& -k_x x_e^2 - k_\theta \sin^2\theta_e - k_\psi \sin^2\psi_e + vy_e \\ &+ (u_R(1-\cos\psi_e)\cos\theta\sin\theta_R + w)z_e + (u_e + e_u)x_e \\ &+ (q_e + e_q)\sin\theta_e + ((r_e + e_r)\sin\psi_e)\cos\theta \\ &+ m_{11}S_u\dot{S}_u + m_{55}S_q\dot{S}_q + m_{66}S_r\dot{S}_r \\ &+ e_u\dot{e}_u + e_q\dot{e}_q + e_r\dot{e}_r \\ &+ \tilde{\boldsymbol{x}}_2^{\mathrm{T}}\hat{\boldsymbol{M}}_I(\boldsymbol{x}_1)\dot{\tilde{\boldsymbol{x}}}_2 + \sum_{i\in S}\tilde{\gamma}_{2i}\dot{\tilde{\gamma}}_{2i} \end{aligned} \quad (46)$$

From the definition of functions $f(x)$ and $g(x)$, $f(x)+g(x) = |x|$ and $f(x) - g(x) = x$. If the upper and lower bounds of the neuron activity are equal (i.e. $B_{(\cdot)} = D_{(\cdot)}$), the bioinspired filter (35) become as follows

$$\begin{cases} \dot{\delta}_u^* = -(A_u + |\delta_u|)\delta_u^* + B_u\delta_u \\ \dot{\delta}_q^* = -(A_q + |\delta_q|)\delta_q^* + B_q\delta_q \\ \dot{\delta}_r^* = -(A_r + |\delta_r|)\delta_r^* + B_r\delta_r \end{cases} \quad (47)$$

Then, the dynamic equations of the error variables e_u, e_q and e_r are derived

$$\begin{cases} \dot{e}_u = -(A_u + |\delta_u|)\delta_u^* + B_u\delta_u - \dot{\delta}_u \\ \dot{e}_q = -(A_q + |\delta_q|)\delta_q^* + B_q\delta_q - \dot{\delta}_q \\ \dot{e}_r = -(A_r + |\delta_r|)\delta_r^* + B_r\delta_r - \dot{\delta}_r \end{cases} \quad (48)$$

Substituting Eqs. (38), (40) and (44), the derivative of the control Lyapunov function (45) can become as follows

$$\begin{aligned}\dot{V}_{all} \le& -\eta_u|S_u| - \eta_q|S_q| - \eta_r|S_r| - l_1x_e^2 - \lambda_y y_e^2 - \lambda_z z_e^2 \\ &- l_2(1-\cos\theta_e) - l_3(1-\cos\psi_e) - l_4e_u^2 - l_5e_q^2 - l_6e_r^2 \\ &- \sum_{i\in S}\sqrt{\frac{2\sigma_{2i}^2}{\hat{m}_{ii}}}V_{o2}^{\frac{1}{2}} + \Delta_1 \\ =& -\xi_1 V_{kin} - \eta_u|S_u| - \eta_q|S_q| - \eta_r|S_r| - l_4e_u^2 \\ &- l_5e_q^2 - l_6e_r^2\sum_{i\in S}\sqrt{\frac{2\sigma_{2i}^2}{\hat{m}_{ii}}}V_{o2}^{\frac{1}{2}} + \Delta_1 \end{aligned} \quad (49)$$

$$\begin{aligned}\dot{V}_{all} \le& -\xi_1 V_{kin} - \frac{\eta_u\mu_7}{2}S_u^2 - \frac{\eta_q\mu_8}{2}S_q^2 - \frac{\eta_r\mu_9}{2}S_r^2 \\ &- \mu_{10}\sum_{i\in S}\sqrt{\frac{2\sigma_{2i}^2}{\hat{m}_{ii}}}V_{o2} - l_4e_u^2 - l_5e_q^2 - l_6e_r^2 + \Delta_2 \\ \le& -\xi_2 V_{all} + \Delta_2 \end{aligned} \quad (50)$$

where the definitions of the above parameters are:

$$\begin{aligned}\Delta_1 =& \frac{1}{2\mu_1}\Psi_u^2 + \frac{1}{2\mu_2}\Psi_q^2 + \frac{1}{2\mu_3}\Psi_r^2 + \frac{1}{2\mu_4}u_e^2 + \frac{1}{2\mu_5}q_e^2 \\ &+ \frac{1}{2\mu_6}r_e^2 + \frac{1}{2}(u_R(1-\cos\psi_e)\cos\theta\sin\theta_R + w)^2 + \frac{1}{2}v^2 \\ &+ (\lambda_y + \frac{1}{2})y_e^2 + (\lambda_z + \frac{1}{2})z_e^2 \\ &+ \sum_{i\in S}(\sqrt{\frac{\sigma_{2i}^2}{\hat{m}_{ii}}}|\tilde{\gamma}_{2i}| + \varepsilon_{0i}\tilde{\gamma}_{2i}\hat{\gamma}_{2i}); \\ l_1 =& k_x - \frac{\mu_4}{2}, \quad l_2 = k_\theta - \frac{\mu_5}{2}, \\ l_3 =& k_\psi - \frac{\mu_6}{2\cos^2\theta}, \quad l_4 = B_u - \frac{\mu_1}{2}, \\ l_5 =& B_q - \frac{\mu_2}{2}, \quad l_6 = B_r - \frac{\mu_3}{2}; \\ \xi_1 =& \min(2l_1, 2\lambda_y, 2\lambda_z, l_2, l_3); \\ \Delta_2 =& \frac{1}{2\mu_1}\Psi_u^2 + \frac{1}{2\mu_2}\Psi_q^2 + \frac{1}{2\mu_3}\Psi_r^2 + \frac{1}{2\mu_4}u_e^2 + \frac{1}{2\mu_5}q_e^2 \\ &+ \frac{1}{2\mu_6}r_e^2 + \frac{1}{2}(u_R(1-\cos\psi_e)\cos\theta\sin\theta_R + w)^2 + \frac{1}{2}v^2 \\ &+ (\lambda_y + \frac{1}{2})y_e^2 + (\lambda_z + \frac{1}{2})z_e^2 \\ &+ \sum_{i\in S}(\sqrt{\frac{\sigma_{2i}^2}{\hat{m}_{ii}}}|\tilde{\gamma}_{2i}| + \varepsilon_{0i}\tilde{\gamma}_{2i}\hat{\gamma}_{2i}) \\ &\frac{1}{2\mu_7} + \frac{1}{2\mu_8} + \frac{1}{2\mu_9} + \frac{1}{2\mu_{10}} \\ \xi_2 =& \min(\xi_1, \eta_u\mu_7, \eta_q\mu_8, \eta_r\mu_9, 2l_4, 2l_5, 2l_6, \mu_{10} \\ &\times\sum_{i\in S}\sqrt{\frac{2\sigma_{2i}^2}{\hat{m}_{ii}}}) \end{aligned}$$

And the symbols μ_i $(i = 1, \ldots, 10)$, λ_y and λ_z are all positive constants to be determined. The notation Ψ_u, Ψ_q and Ψ_r are

$$\Psi_u = x_e - \dot{\delta}_u, \quad \Psi_q = \sin\theta_e - \dot{\delta}_q, \quad \Psi_r = \sin\psi_e/\cos\theta - \dot{\delta}_r$$

From Eq.(50), it can be seen that all tracking error variables x_e, y_e, z_e, θ_e, ψ_e, $\hat{u}_e$, $\hat{q}_e$, $\hat{r}_e$, e_u, e_q and e_r are stabilized to the bounded neighborhood of the origin. ■

IV. NUMERICAL SIMULATIONS

In this section, the proposed spatial output-feedback trajectory tracking control scheme is applied to the 5-DOF motion model of the underactuated UUV shown in section II.

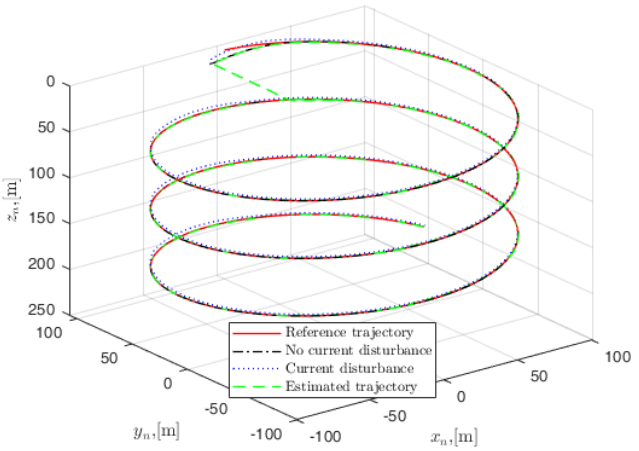

FIGURE 2. Helical trajectory tracking, UUV predefined reference trajectory (solid line), actual trajectory without current disturbance (dashdot line), actual trajectory with current disturbance (dotted line), and estimated trajectory (dashed line).

The typical numerical simulation results are provided to demonstrate that the designed output-feedback trajectory tracking controller can effectively force an underactuated UUV to track the desired spatial trajectories, and is robust to parameter perturbations and unknown ocean currents. The nominal values of hydrodynamic parameters of the simulation model are given in the table: [54]

TABLE 1. Rigid body parameters and nominal values of hydrodynamic parameters.

Signification	Parameter and Value
inertia terms	$\hat{m}_{11}=215$ kg , $\hat{m}_{22}=265$ kg , $\hat{m}_{33}=265$ kg , $\hat{m}_{55}=80$ kg$\cdot$m^2 , $\hat{m}_{66}=80$ kg$\cdot$m^2
linear drag hydrodynamic coefficient terms	$\hat{X}_u=70$ kg/s , $\hat{Y}_v=100$ kg/s , $\hat{Z}_w=100$ kg/s , $\hat{M}_q=50$ kg$\cdot$m^2/s , $\hat{N}_r=50$ kg$\cdot$m^2/s
quadratic drag hydrodynamic coefficient terms	$\hat{X}_{u\|u\|}=100$ kg/m , $\hat{Y}_{v\|v\|}=200$ kg/m , $\hat{Z}_{w\|w\|}=200$ kg/m , $\hat{M}_{q\|q\|}=100$ kg$\cdot$m^2 , $\hat{N}_{r\|r\|}=100$ kg$\cdot$m^2
rigid body parameter	$m=185$ kg , $W=1813$ N , $B=1813$ N , $z_G=0.1$ m , $z_B=-0.1$ m

To illustrate the robustness of the trajectory tracking controller, the simulation motion model is added the ±20% parameter perturbation in all hydrodynamic coefficients. In one of the numerical simulations, the constant ocean currents with speed 0.75 m/s and direction 60° is introduced to the kinetic equations(4), which is used to reveal the robustness concerning the ocean currents. The kinetic equations (4) become as follows [33]:

$$\begin{cases} m_{11}\dot{u} = m_{22}v_r r - m_{33}w_r q - X_u u_r - X_{u|u|}u_r\,|u_r| + \tau_1 \\ m_{22}\dot{v} = -m_{11}u_r r - Y_v v_r - Y_{v|v|}v_r\,|v_r| \\ m_{33}\dot{w} = m_{11}u_r q - Z_w w_r - Z_{w|w|}w_r\,|w_r| \\ m_{55}\dot{q} = (m_{33}-m_{11})u_r w_r - M_q q - M_{q|q|}q\,|q| \\ \qquad -(z_G W - z_B B)\sin\theta + \tau_5 \\ m_{66}\dot{r} = (m_{11}-m_{22})u_r v_r - N_r r - N_{r|r|}r\,|r| + \tau_6 \end{cases} \tag{51}$$

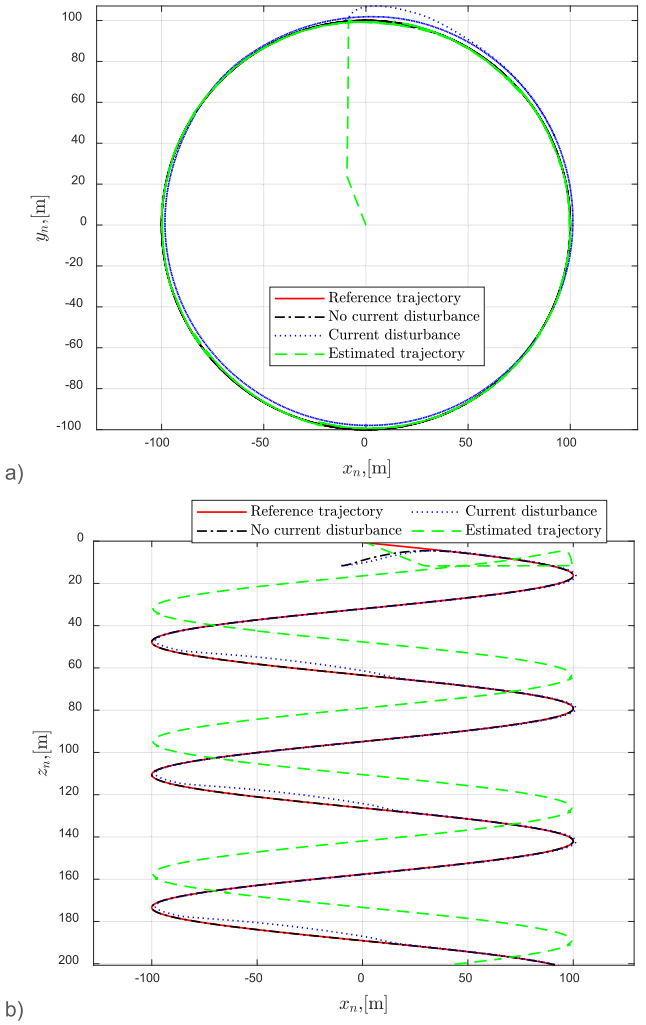

FIGURE 3. The projection of the spatial trajectory tracking results: a) $o_n x_n y_n$ projection, b) $o_n x_n z_n$ projection.

where, $u_r = u - u_c$, $v_r = v - v_c$ and $w_r = w - w_c$ are the relative velocities. The symbols u_c, v_c and w_c are ocean current velocity in $\{b\}$, which are summed up $\nu_c^b = [u_c, v_c, w_c]^{\mathrm{T}}$. The ocean current velocity vector $\boldsymbol{\nu}_c^b$ can be obtained

$$\boldsymbol{\nu}_c^b = \mathbf{R}_b^n(\boldsymbol{\Theta}_{nb})^{-1}\boldsymbol{\nu}_c^n \tag{52}$$

where, $\boldsymbol{\nu}_c^n = [V_c\cos(\beta_c), V_c\sin(\beta_c), 0]^{\mathrm{T}}$ is the ocean current velocity vector in $\{n\}$, V_c and β_c are the ocean speed and direction in $\{n\}$. Then, the ocean current velocity vector ν_c^n is equal to $\nu_c^n = [0.38\mathrm{m/s}, 0.65\mathrm{m/s}, 0\mathrm{m/s}]^{\mathrm{T}}$. In all of following simulations, the identical output-feedback trajectory tracking controller is adopted to force the underactuated UUV to track the spatial desired reference trajectory. The gain coefficients of the equivalent output injection SMO are set as follows: $\gamma_{11}=8, \gamma_{12}=20, \gamma_{13}=8, \gamma_{15}=0.1, \gamma_{16}=1.8, \varepsilon_{01}=0.5, \varepsilon_{02}=0.5, \varepsilon_{03}=0.5, \varepsilon_{05}=0.1, \varepsilon_{06}=0.1, \varepsilon_{11}=1, \varepsilon_{12}=1, \varepsilon_{13}=1, \varepsilon_{15}=4, \varepsilon_{16}=8$ and $\mathrm{T}_{0i}=0.04$ $(i=1,2,3,5,6)$. The gain coefficients of the designed tracking controller are set as follows: $k_x=0.6$, $k_\theta=4.9$, $k_\psi=3.9$, $A_j=0.08$,

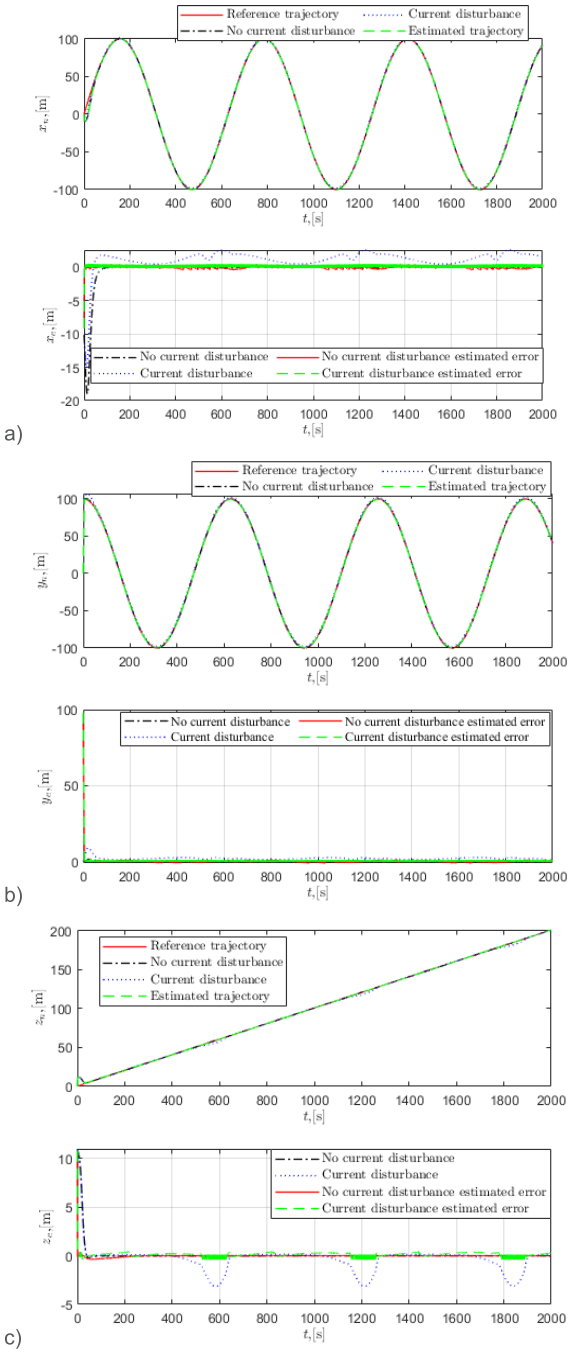

FIGURE 4. The tracking response for the position of the underactuated UUV and their tracking errors: a) x_n- axes tracking response and error, b) y_n-axes tracking response and error, c) z_n-axes tracking response and error.

$B_j = 0.5$, $C_j = 0.3$ $(i = u, q, r)$, $\hat{\lambda}_u = 0.8$, $\hat{\lambda}_q = 0.7$, $\hat{\lambda}_u = 0.6$, $\hat{\alpha}_1 = 0.1$, $\hat{\alpha}_5 = 0.12$, $\hat{\alpha}_6 = 0.2$, $\hat{\eta}_u = 0.1$, $\hat{\eta}_q = 0.8$ and $\hat{\eta}_r = 0.5$. In all simulations, the predefined reference trajectory is the helical trajectory in the inertial reference frame $\{n\}$, and is described as:

$$\begin{cases} x_{\mathrm{R}} = 100\sin(0.01t) \\ y_{\mathrm{R}} = 100\cos(0.01t) \\ z_{\mathrm{R}} = 0.1t + 0.6 \end{cases} \tag{53}$$

Under the spatial output-feedback trajectory tracking controller (32), (35) and (44), the underactuated UUV starts from the stationary state. The initial position and attitude of the UUV are $x = -10$ m, $y = 100$ m, $z = 11.6$ m, $\theta = 0^\circ$ and $\psi = 0^\circ$. The numerical simulation results are shown in Fig. 2 to Fig.8. The actual, estimated and desired trajectories in the underwater three-dimensional space are displayed in Fig. 2, and their projections in the $o_n x_n y_n$ and $o_n x_n z_n$ are shown in Fig.3. The tracking response and errors of the position for the underactuated UUV in $\{n\}$ are demonstrated in Fig.4. These simulation results indicate that the estimation position and the actual position of the underactuated UUV can quickly converge to the desired reference trajectory. The absolute values of the tracking and estimated errors without current disturbance are less than 0.13m, 0.95m, 0.01m (x_e, y_e, z_e) and 0.39m, 0.41m, 0.2m $(\tilde{x}, \tilde{y}, \tilde{z})$, and their absolute values with current are 2.6m, 2.63m, 3.14m (x_e, y_e, z_e) and 0.42m, 0.46m, 0.31m $(\tilde{x}, \tilde{y}, \tilde{z})$. In Fig.5, the tracking response and errors of the attitude angle are revealed. When the current disturbance exist, it can be seen from Fig.4 that the pitch angle θ appears -20° limit pitch angle for a long time, and the yaw also has $\pm 50^\circ$ tracking error (more than 300° yaw angular error is mainly due to the jump of the yaw angle at $\pm 180^\circ$).

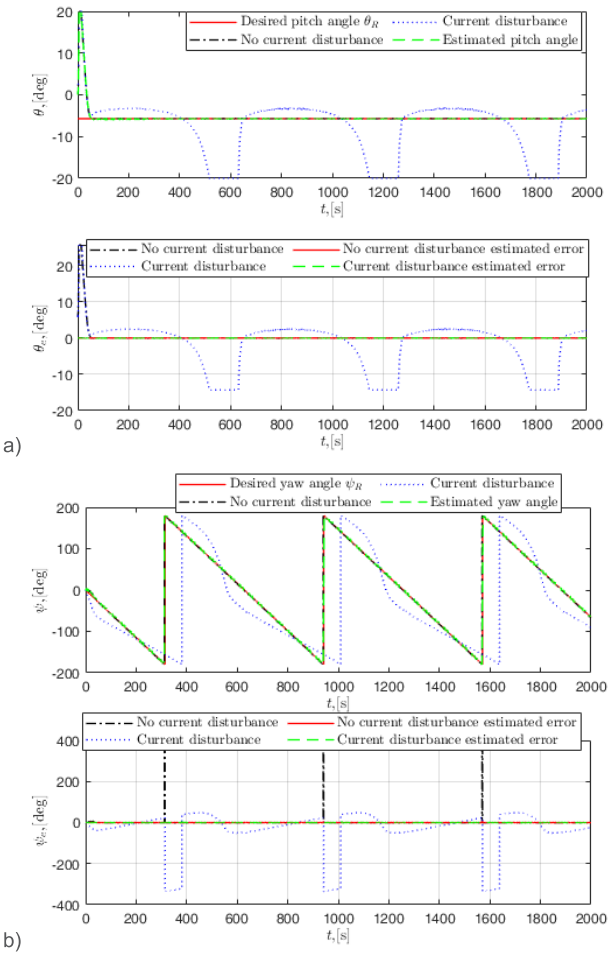

FIGURE 5. a) The tracking response of the pitch angle θ and its tracking error, b) The tracking response of the yaw angle ψ and its tracking error.

The attitude tracking errors are almost zero without current disturbance. The estimated errors all are almost zero.

Fig.6 shows the tracking responses of the linear velocities and their tracking errors. Due to the initial position-tracking error, there is a significant transient process in the tracking response of the surge velocity. When the current disturbances exist, there are some certain errors in the tracking responses of all linear velocities. The absolute values of the linear velocity tracking errors and estimated errors without current all are less than 0.03 m/s, while these linear velocity tracking errors and estimated errors under current are -0.35 m/s $\leq u_e \leq$ 0 m/s, $|\tilde{u}| \leq 0.80$ m/s, $|v_e| \leq 0.75$ m/s, $|\tilde{v}| \leq 0.75$ m/s, -0.30 m/s $\leq w_e \leq 0.13$ m/s and -0.35 m/s $\leq \tilde{w} \leq$ 0.17 m/s. When the underactuated UUV with current disturbance changes its depth, its heave velocity comes into being spikes. Compared to the no-current disturbances, all linear velocities of the UUV have large tracking errors under the current disturbances, especially yaw and heave velocity.

The tracking response of the pitch and yaw angular velocities and their tracking errors are displayed in Fig.7. The tracking errors and estimated errors of the pitch and yaw angular velocities without current meet the following conditions: $|q_e| \leq 0.002$ rad/s, $|r_e| \leq 0.005$ rad/s, $|\tilde{q}| \leq 0.003$ rad/s and $|\tilde{r}| \leq 0.004$ rad/s, respectively, while the pitch and yaw angular velocity with current appears the maximum angular velocity tracking error of -0.1 rad/s and -0.026 rad/s, respectively. Simultaneously, there is a certain fluctuation in the estimated value of yaw angular velocity. Fig.8 shows the control inputs of the underactuated UUV, including the surge control force τ_1, the pitch control torque τ_5 and the yaw control torque τ_6.

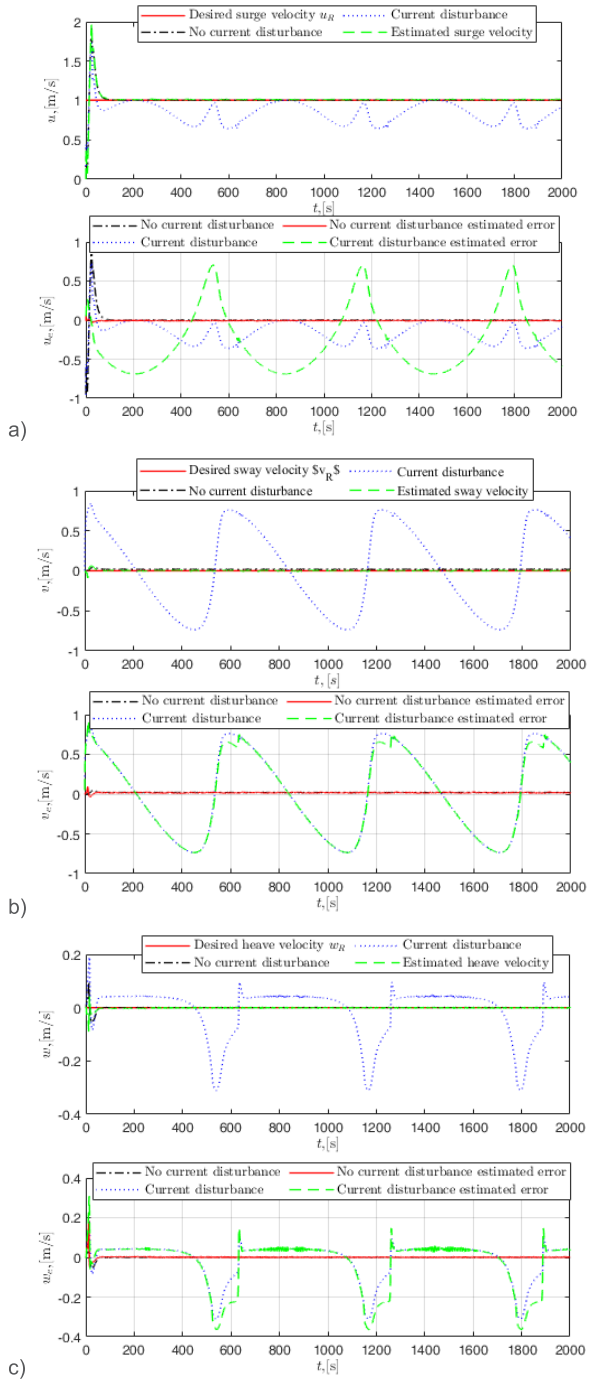

FIGURE 6. a) The tracking response of the surge velocity *u* and its tracking error, b) The tracking response of the sway velocity *v* and its tracking error, c) The tracking response of the heave velocity *w* and its tracking error.

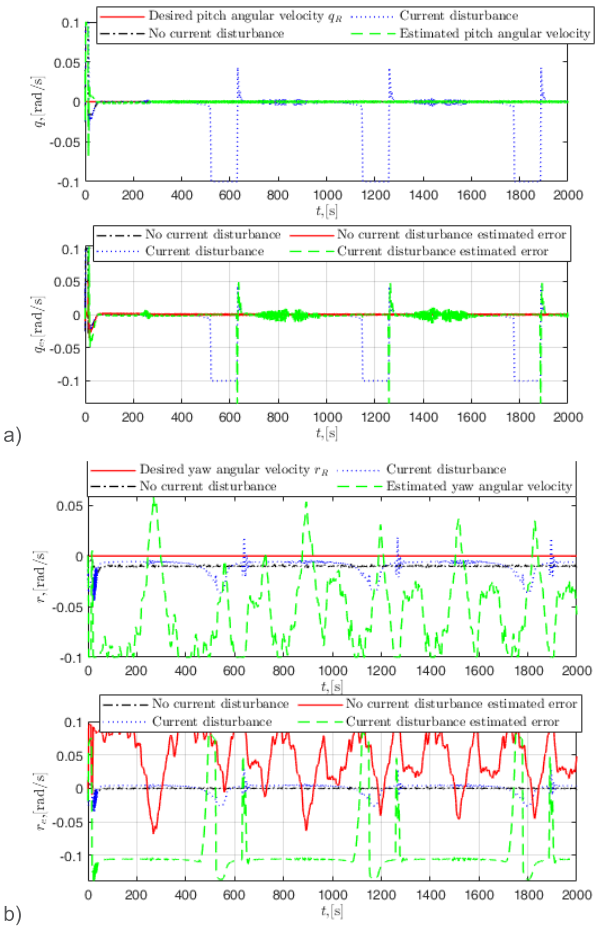

FIGURE 7. a) The tracking response of the pitch angular velocity *q* and its tracking error, b) The tracking response of the yaw angular velocity *r* and its tracking error.

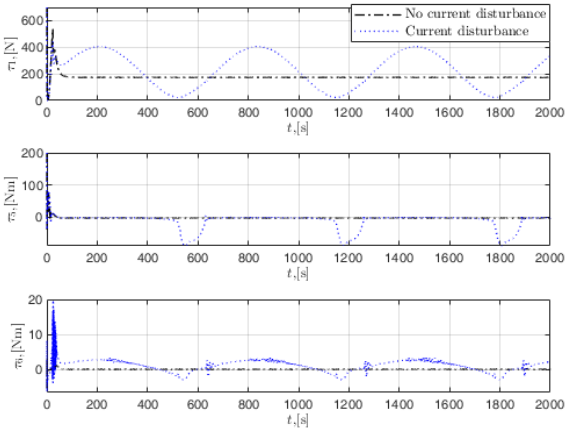

FIGURE 8. The surge control force τ_1, the pitch control torque τ_5 and the yaw control torque τ_6.

V. CONCLUSION

This work addressed the tracking problems of the spatial trajectory for underactuated UUVs without linear and angular velocity measurements. Firstly, the state-feedback tracking controller has been developed based the bioinspired filtering backstepping and first-order integral SMC. To obtain the velocity information (including linear and angular velocities) for feedback, a finite-time convergent observer has been proposed in the light of the equivalent output injection SMO, to reconstruct the full motion states of underactuated UUVs in the three-dimensional underwater space. Well, the spatial output-feedback trajectory tracking control scheme has been designed by combining the corresponding the state-feedback tracking controller and the finite-time convergent motion state observer together. The proposed output-feedback trajectory tracking controller is strongly robust with regard to model parameter perturbation and constant unknown current, and stabilize all tracking errors to the bounded neighborhood of the origin. All analysis results show that the proposed tracking control scheme is provided with the preferably control performance.

REFERENCES

[1] J. Yuh, "Design and control of autonomous underwater robots: A survey," *Auton. Robots*, vol. 8, no. 1, pp. 7–24, Jan. 2000.

[2] A. Sahoo, S. K. Dwivedy, and P. S. Robi, "Advancements in the field of autonomous underwater vehicle," *Ocean Eng.*, vol. 181, pp. 145–160, Jun. 2019.

[3] F. Repoulias and E. Papadopoulos, "Planar trajectory planning and tracking control design for underactuated AUVs," *Ocean Eng.*, vol. 34, nos. 11–12, pp. 1650–1667, Aug. 2007.

[4] Z. Yan, H. Yu, W. Zhang, B. Li, and J. Zhou, "Globally finite-time stable tracking control of underactuated UUVs," *Ocean Eng.*, vol. 107, pp. 132–146, Oct. 2015.

[5] A. A. R. Al Makdah, N. Daher, D. Asmar, and E. Shammas, "Three-dimensional trajectory tracking of a hybrid autonomous underwater vehicle in the presence of underwater current," *Ocean Eng.*, vol. 185, pp. 115–132, Aug. 2019.

[6] C. Paliotta, E. Lefeber, K. Y. Pettersen, J. Pinto, M. Costa, and J. T. de Figueiredo Borges de Sousa, "Trajectory tracking and path following for underactuated marine vehicles," *IEEE Trans. Control Syst. Technol.*, vol. 27, no. 4, pp. 1423–1437, Jul. 2019.

[7] Z. Peng, J. Wang, and J. Wang, "Constrained control of autonomous underwater vehicles based on command optimization and disturbance estimation," *IEEE Trans. Ind. Electron.*, vol. 66, no. 5, pp. 3627–3635, May 2019.

[8] X. Liang, X. Qu, Y. Hou, and Q. Ma, "Three-dimensional trajectory tracking control of an underactuated autonomous underwater vehicle based on ocean current observer," *Int. J. Adv. Robot. Syst.*, vol. 15, no. 5, Oct. 2018, Art. no. 172988141880681.

[9] S. Li, X. Wang, and L. Zhang, "Finite-time output feedback tracking control for autonomous underwater vehicles," *IEEE J. Ocean. Eng.*, vol. 40, no. 3, pp. 727–751, Jul. 2015.

[10] H. Yu, C. Guo, and Z. Yan, "Globally finite-time stable three-dimensional trajectory-tracking control of underactuated UUVs," *Ocean Eng.*, vol. 189, Oct. 2019, Art. no. 106329.

[11] S. A. Gafurov and E. V. Klochkov, "Autonomous unmanned underwater vehicles development tendencies," *Procedia Eng.*, vol. 106, pp. 141–148, 2015.

[12] M. Khalid, Z. Ullah, N. Ahmad, M. Arshad, B. Jan, Y. Cao, and A. Adnan, "A survey of routing issues and associated protocols in underwater wireless sensor networks," *J. Sensors*, vol. 2017, May 2017, Art. no. 7539751.

[13] K. Y. Wichlund, O. J. Sordalen, and O. Egeland, "Control properties of underactuated vehicles," in *Proc. IEEE Int. Conf. Robot. Automat.*, Nagoya, Japan, May 1995, pp. 2009–2014.

[14] K. D. Do and J. Pan, "Underactuated ships follow smooth paths with integral actions and without velocity measurements for feedback: Theory and experiments," *IEEE Trans. Control Syst. Technol.*, vol. 14, no. 2, pp. 308–322, Mar. 2006.

[15] R. W. Brockett, "Asymptotic stability and feedback stabilization," in *Differential Geometric Control Theory*, vol. 1, R. W. Brockett, R. S. Millman, and H. J. Sussmann, Eds. Boston, MA, USA: Birkhäuser, 1983, pp. 181–191.

[16] J.-B. Pomet, "Explicit design of time-varying stabilizing control laws for a class of controllable systems without drift," *Syst. Control Lett.*, vol. 18, no. 2, pp. 147–158, Feb. 1992.

[17] A. P. Aguiar and J. P. Hespanha, "Trajectory-tracking and path-following of underactuated autonomous vehicles with parametric modeling uncertainty," *IEEE Trans. Autom. Control*, vol. 52, no. 8, pp. 1362–1379, Aug. 2007.

[18] F. Rezazadegan, K. Shojaei, F. Sheikholeslam, and A. Chatraei, "A novel approach to 6-DOF adaptive trajectory tracking control of an AUV in the presence of parameter uncertainties," *Ocean Eng.*, vol. 107, pp. 246–258, Oct. 2015.

[19] Y. Chen, R. Zhang, X. Zhao, and J. Gao, "Adaptive fuzzy inverse trajectory tracking control of underactuated underwater vehicle with uncertainties," *Ocean Eng.*, vol. 121, pp. 123–133, Jul. 2016.

[20] T. Elmokadem, M. Zribi, and K. Youcef-Toumi, "Trajectory tracking sliding mode control of underactuated AUVs," *Nonlinear Dyn.*, vol. 84, no. 2, pp. 1079–1091, Apr. 2016.

[21] Y. Wang, L. Gu, M. Gao, and K. Zhu, "Multivariable output feedback adaptive terminal sliding mode control for underwater vehicles," *Asian J. Control*, vol. 18, no. 1, pp. 247–265, Nov. 2016.

[22] C. P. Bechlioulis, G. C. Karras, S. Heshmati-Alamdari, and K. J. Kyriakopoulos, "Trajectory tracking with prescribed performance for underactuated underwater vehicles under model uncertainties and external disturbances," *IEEE Trans. Control Syst. Technol.*, vol. 25, no. 2, pp. 429–440, Mar. 2017.

[23] T. Elmokadem, M. Zribi, and K. Youcef-Toumi, "Terminal sliding mode control for the trajectory tracking of underactuated autonomous underwater vehicles," *Ocean Eng.*, vol. 129, pp. 613–625, Jan. 2017.

[24] S. Liu, Y. Liu, and N. Wang, "Nonlinear disturbance observer-based backstepping finite-time sliding mode tracking control of underwater vehicles with system uncertainties and external disturbances," *Nonlinear Dyn.*, vol. 88, no. 1, pp. 465–476, Apr., 2017.

[25] X. Liang, X. Qu, L. Wan, and Q. Ma, "Three-dimensional path following of an underactuated AUV based on fuzzy backstepping sliding mode control," *Int. J. Fuzzy Syst.*, vol. 20, no. 2, pp. 640–649, Feb., 2018.

[26] L. Qiao and W. Zhang, "Adaptive second-order fast nonsingular terminal sliding mode tracking control for fully actuated autonomous underwater vehicles," *IEEE J. Ocean. Eng.*, vol. 44, no. 2, pp. 363–385, Apr. 2019.

[27] F. S. Tabataba'i-Nasab, A. Keymasi Khalaji, and S. A. A. Moosavian, "Adaptive nonlinear control of an autonomous underwater vehicle," *Trans. Inst. Meas. Control*, vol. 41, no. 11, pp. 3121–3131, Jul. 2019.

[28] K. D. von Ellenrieder, "Dynamic surface control of trajectory tracking marine vehicles with actuator magnitude and rate limits," *Automatica*, vol. 105, pp. 433–442, Jul. 2019.

[29] Z. Yan, M. Wang, and J. Xu, "Integrated guidance and control strategy for homing of unmanned underwater vehicles," *J. Franklin Inst.*, vol. 356, no. 7, pp. 3831–3848, May 2019.

[30] Z. Yan, M. Wang, and J. Xu, "Global adaptive neural network control of underactuated autonomous underwater vehicles with parametric modeling uncertainty," *Asian J. Control*, vol. 21, no. 3, pp. 1342–1354, May 2019.
[31] L. Qiao and W. Zhang, "Trajectory tracking control of AUVs via adaptive fast nonsingular integral terminal sliding mode control," *IEEE Trans Ind. Informat.*, vol. 16, no. 2, pp. 1248–1258, Oct., 2019.
[32] L. Qiao and W. Zhang, "Double-loop integral terminal sliding mode tracking control for UUVs with adaptive dynamic compensation of uncertainties and disturbances," *IEEE J. Ocean. Eng.*, vol. 44, no. 1, pp. 29–53, Jan. 2019.
[33] T. I. Fossen, *Handbook of Marine Craft Hydrodynamics and Motion Control*. Chichester, U.K.: Wiley, 2011.
[34] S. Ding, W.-H. Chen, K. Mei, and D. J. Murray-Smith, "Disturbance observer design for nonlinear systems represented by input–output models," *IEEE Trans. Ind. Electron.*, vol. 67, no. 2, pp. 1222–1232, Feb. 2020.
[35] L. Fang, L. Ma, S. Ding, and D. Zhao, "Finite-time stabilization for a class of high-order stochastic nonlinear systems with an output constraint," *Appl. Math. Comput.*, vol. 358, pp. 63–79, Oct. 2019.
[36] Y. Wang, J. Chen, and L. Gu, "Output feedback fractional-order nonsingular terminal sliding mode control of underwater remotely operated vehicles," *Sci. World J.*, vol. 2014, pp. 1–19, May., 2014.
[37] J. M. Daly and D. W. L. Wang, "Output feedback sliding mode control in the presence of unknown disturbances," *Syst. Control Lett.*, vol. 58, no. 3, pp. 188–193, Mar. 2009.
[38] D. Zhao, S. Li, and Q. Zhu, "Output feedback terminal sliding mode control for a class of second order nonlinear systems," *Asian J. Control*, vol. 15, no. 1, pp. 237–247, Feb. 2013.
[39] Z. Jia, Z. Hu, and W. Zhang, "Adaptive output-feedback control with prescribed performance for trajectory tracking of underactuated surface vessels," *ISA Trans.*, vol. 95, pp. 18–26, Dec. 2019.
[40] V. I. Utkin, "Sliding mode control design principles and applications to electric drives," *IEEE Trans. Ind. Electron.*, vol. 40, no. 1, pp. 23–36, Feb. 1993.
[41] C. Edwards, and S. K. Spurgeon, *Sliding Mode Control: Theory And Applications*. London, U.K.: Taylor & Francis, 1998.
[42] Z.-P. Yan, H.-M. Yu, and S.-P. Hou, "Diving control of underactuated unmanned undersea vehicle using integral-fast terminal sliding mode control," *J. Central South Univ.*, vol. 23, no. 5, pp. 1085–1094, May 2016.
[43] M. Zak, "Terminal attractors for addressable memory in neural networks," *Phys. Lett. A*, vol. 133, nos. 1–2, pp. 18–22, Oct. 1988.
[44] Y. Feng, X. Yu, and Z. Man, "Non-singular terminal sliding mode control of rigid manipulators," *Automatica*, vol. 38, no. 12, pp. 2159–2167, Dec. 2002.
[45] X. Yu and M. Zhihong, "Fast terminal sliding-mode control design for nonlinear dynamical systems," *IEEE Trans. Circuits Syst. I, Fundam. Theory Appl.*, vol. 49, no. 2, pp. 261–264, Feb. 2002.
[46] C.-S. Chiu, "Derivative and integral terminal sliding mode control for a class of MIMO nonlinear systems," *Automatica*, vol. 48, no. 2, pp. 316–326, Feb. 2012.
[47] C. Yu, C. Liu, L. Lian, X. Xiang, and Z. Zeng, "ELOS-based path following control for underactuated surface vehicles with actuator dynamics," *Ocean Eng.*, vol. 187, Sep. 2019, Art. no. 106139.
[48] Z. Yuguang and Y. Fan, "Dynamic modeling and adaptive fuzzy sliding mode control for multi-link underwater manipulators," *Ocean Eng.*, vol. 187, Sep. 2019, Art. no. 106202.
[49] I. Haskara, "On sliding mode observers via equivalent control approach," *Int. J. Control*, vol. 71, no. 6, pp. 1051–1067, Nov. 1998.
[50] H. Ho Choi, "Sliding-mode output feedback control design," *IEEE Trans. Ind. Electron.*, vol. 55, no. 11, pp. 4047–4054, Nov. 2008.
[51] S. K. Spurgeon, "Sliding mode observers: A survey," *Int. J. Syst. Sci.*, vol. 39, no. 8, pp. 751–764, Aug. 2008.
[52] B. Bandyopadhyay, P. S. Gandhi, and S. Kurode, "Sliding mode observer based sliding mode controller for slosh-free motion through PID scheme," *IEEE Trans. Ind. Electron.*, vol. 56, no. 9, pp. 3432–3442, Sep. 2009.
[53] Y. Wang, F. Yan, J. Chen, F. Ju, and B. Chen, "A new adaptive time-delay control scheme for cable-driven manipulators," *IEEE Trans Ind. Informat.*, vol. 15, no. 6, pp. 3469–3481, Jun. 2019.
[54] K. Y. Pettersen and O. Egeland, "Time-varying exponential stabilization of the position and attitude of an underactuated autonomous underwater vehicle," *IEEE Trans. Autom. Control*, vol. 44, no. 1, pp. 112–115, Jan. 1999.
[55] S. X. Yang, A. Zhu, G. Yuan, and M. Q. Meng, "A bioinspired neurodynamics-based approach to tracking control of mobile robots," *IEEE Trans. Ind. Electron.*, vol. 59, no. 8, pp. 3211–3220, Aug. 2012.
[56] B. Sun, D. Zhu, and S. X. Yang, "A bioinspired filtered backstepping tracking control of 7000-m manned submarine vehicle," *IEEE Trans. Ind. Electron.*, vol. 61, no. 7, pp. 3682–3693, Jul. 2014.
[57] C. Pan, X. Lai, S. X. Yang, and M. Wu, "A bioinspired neural dynamics-based approach to tracking control of autonomous surface vehicles subject to unknown ocean currents," *Neural Comput. Appl.*, vol. 26, no. 8, pp. 1929–1938, Feb. 2015.

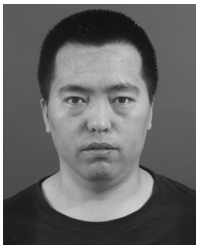

HAOMIAO YU was born in Harbin, China, in 1983. He received the B.S. degree in optical information science and engineering and the Ph.D. degree in control theory and control engineering from Harbin Engineering University, Harbin, in 2008 and 2016, respectively.

He is currently a Lecturer with the College of Marine Electrical Engineering, Dalian Maritime University, Dalian, China. His research interests include the design and development of navigation, guidance and control algorithms for unmanned underwater vehicles and unmanned surface vehicles.

CHEN GUO was born in Rudong, China, in 1956. He received the B.E. degree from Chongqing University, Chongqing, China, in 1982, and the M.S. and Ph.D. degrees in marine engineering automation from Dalian Maritime University, Dalian, China, in 1985 and 1992, respectively.

He is currently a Professor with the College of Marine Electrical Engineering, Dalian Maritime University. His main activities focused on intelligent control, soft computing, and marine system automation and simulation.

ZHIPENG SHEN was born in Fujian, China, in 1977. He received the B.E. and Ph.D. degrees in control engineering from Dalian Maritime University, Dalian, China, in 2000 and 2005, respectively. He is currently a Professor with the College of Marine Electrical Engineering, Dalian Maritime University. His research interests include on the nonlinear control, intelligent control and its application in surface vehicles.

ZHEPING YAN was born in Hangzhou, China, in 1972. He received the B.E. degree in nuclear power plant, the M.S. degree in special auxiliary device and system in naval architecture and ocean engineering, and the Ph.D. degree in control theory and control engineering from Harbin Engineering University, Harbin, China, in 1994, 1997, and 2001, respectively.

He was a Visiting Scholar with the National University of Singapore, Singapore, in 2015, Australian National University, Canberra, Australia, in 2016, and University of Guelph, Guelph, Canada, in 2017. He is currently a Professor with the College of Automation and the Director of Marine Assembly and Automatic Technology Institute, Harbin Engineering University. He is also a Chair Professor with Dalian Maritime University, Dalian, China, and the Deputy Secretary-General of the National Standardization Committee of Submersibles, and the Associate Supervisor of the State Key Laboratory of Underwater Robot Technology. His current research interests include the design and development of systems, cooperative control and motion control algorithms for unmanned underwater vehicles, identification of non-linear systems, and multisensors data fusion and intelligent control.